Climate Change 2013: The Physical Science Basis

Summary for Policymakers

Drafting Authors: Lisa Alexander (Australia), Simon Allen (Switzerland/New Zealand), Nathaniel L. Bindoff (Australia), Francois-Marie Breon (France), John Church (Australia), Ulrich Cubasch (Germany), Seita Emori (Japan), Piers Forster (UK), Pierre Friedlingstein (UK/Belgium), Nathan Gillett (Canada), Jonathan Gregory (UK), Dennis Hartmann (USA), Eystein Jansen (Norway), Ben Kirtman (USA), Reto Knutti (Switzerland), Krishna Kumar Kanikicharla (India), Peter Lemke (Germany), Jochem Marotzke (Germany), Valerie Masson-Delmotte (France), Gerald Meehl (USA), Igor Mokhov (Russia), Shilong Piao (China), Gian-Kasper Plattner (Switzerland), Qin Dahe (China), Venkatachalam Ramaswamy (USA), David Randall (USA), Monika Rhein (Germany), Maisa Rojas (Chile), Christopher Sabine (USA), Drew Shindell (USA), Thomas F. Stocker (Switzerland), Lynne Talley (USA), David Vaughan (UK), Shang-Ping Xie (USA)

Draft Contributing Authors (list will be updated): Myles Allen (UK), Olivier Boucher (France), Don Chambers (USA), Philippe Ciais (France), Peter Clark (USA), Matthew Collins (UK), Josefino Comiso (USA), Richard Feely (USA), Gregory Flato (Canada), Jan Fuglestvedt (Norway), Jens Hesselbjerg Christensen (Denmark), Gregory Johnson (USA), Georg Kaser (Austria), Vladimir Kattsov (Russia), Albert Klein Tank (Netherlands), Corinne Le Quere (UK), Viviane Vasconcellos de Menezes (Australia/Brazil), Gunnar Myhre (Norway), Tim Osborn (UK), Antony Payne (UK), Judith Perlwitz (USA), Scott Power (Australia), Stephen Rintoul (Australia), Joeri Rogelj (Switzerland), Matilde Rusticucci (Argentina), Michael Schulz (Germany), Jan Sedláček (Switzerland), Peter Stott (UK), Rowan Sutton (UK), Peter Thorne (USA/Norway/UK), Donald Wuebbles (USA)

Date of Draft: 7 June 2013

Introduction

The Working Group I contribution to the IPCC's Fifth Assessment Report considers new evidence of past and projected future climate change based on many independent scientific analyses ranging from observations of the climate system, paleoclimate archives, theoretical studies of climate processes and simulations using climate models.

This Summary for Policymakers (SPM) follows the structure of the Working Group I report. The narrative is supported by a series of overarching assessment conclusions highlighted in shaded boxed statements. Main sections of the Summary for Policymakers are introduced with a brief chapeau in italics.

The degree of certainty in key findings in this assessment is based on the author teams' evaluations of underlying scientific understanding and is expressed as a qualitative level of confidence and, when possible, probabilistically with a quantified likelihood. Confidence in the validity of a finding is based on the type, amount, quality, and consistency of evidence (e.g., mechanistic understanding, theory, data, models, expert judgment) and the degree of agreement[1]. Probabilistic estimates of quantified measures of uncertainty in a finding are based on statistical analysis of observations or model results, or expert judgment[2]. Where appropriate, findings are also formulated as statements of fact without using uncertainty qualifiers. (See Chapter 1 and Box TS.1 for more details)

The basis for substantive paragraphs in this Summary for Policymakers can be found in the chapter sections of the underlying report and in the Technical Summary. These references are given in curly brackets.

Observed Changes in the Climate System

Observations of the climate system are based on direct physical and biogeochemical measurements, remote sensing from ground stations and satellites; information derived from paleoclimate archives provides a long-term context. Global-scale observations from the instrumental era began in the mid-19th century, and paleoclimate reconstructions extend the record of some quantities back hundreds to millions of years. Together, they provide a comprehensive view of the variability and long-term changes in the atmosphere, the ocean, the cryosphere, and the land surface.

Since 1950, changes have been observed throughout the climate system: the atmosphere and ocean have warmed, the extent and volume of snow and ice have diminished, and sea level has risen (see Figures SPM.1 and SPM.2). Many of these observed changes are unusual or unprecedented on time scales of decades to millennia. {2.4, 3.2, 3.7, 4.2–4.7, 5.3, 5.5–5.7, 13.2}

[1] In this Summary for Policymakers, the following summary terms are used to describe the available evidence: limited, medium, or robust; and for the degree of agreement: low, medium, or high. A level of confidence is expressed using five qualifiers: very low, low, medium, high, and very high, and typeset in italics, e.g., *medium confidence*. For a given evidence and agreement statement, different confidence levels can be assigned, but increasing levels of evidence and degrees of agreement are correlated with increasing confidence (see Chapter 1 and Box TS.1 for more details).

[2] In this Summary for Policymakers, the following terms have been used to indicate the assessed likelihood of an outcome or a result: virtually certain 99–100% probability, very likely 90–100%, likely 66–100%, about as likely as not 33–66%, unlikely 0–33%, very unlikely 0–10%, exceptionally unlikely 0–1%. Additional terms (extremely likely: 95–100%, more likely than not >50–100%, and extremely unlikely 0–5%) may also be used when appropriate. Assessed likelihood is typeset in italics, e.g., *very likely* (see Chapter 1 and Box TS.1 for more details).

Atmosphere

Each of the last three decades has been warmer than all preceding decades since 1850 and the first decade of the 21st century has been the warmest (see Figure SPM.1). Analyses of paleoclimate archives indicate that in the Northern Hemisphere, the period 1983–2012 was *very likely* the warmest 30-year period of the last 800 years (*high confidence*) and *likely* the warmest 30-year period of the last 1400 years (*medium confidence*). {2.4, 5.3}

[INSERT FIGURE SPM.1 HERE]
Figure SPM.1: (a) Observed global mean combined land and ocean temperature anomalies from three surface temperature data sets (black – HadCRUT4, yellow – MLOST, blue – GISS). Top panel: annual mean values, bottom panel: decadal mean values including the estimate of uncertainty for HadCRUT4. Anomalies are relative to the mean of 1961−1990. (b) Map of the observed temperature change from 1901−2012derived from temperature trends determined by linear regression of the MLOST time series. Trends have been calculated only for grid boxes with greater than 70% complete records and more than 20% data availability in the first and last 10% of the time period. Grid boxes where the trend is significant at the 10% level are indicated by a + sign. {Figures 2.19–2.21; Figure TS.2}

- The globally averaged combined land and ocean surface temperature data show an increase of 0.89 [0.69 to 1.08] °C [3] over the period 1901–2012. Over this period almost the entire globe has experienced surface warming. (Figure SPM.1). {2.4.3}

- Global mean surface temperature trends exhibit substantial decadal variability, despite the robust multi-decadal warming since 1901 (Figure SPM 1). The rate of warming over the past 15 years (1998−2012; 0.05 [−0.05 to +0.15] °C per decade) is smaller than the trend since 1951 (1951−2012; 0.12 [0.08 to 0.14] °C per decade). (Figure SPM.1) {2.4.3}

- Continental-scale surface temperature reconstructions show, with *high confidence*, multi-decadal intervals during the Medieval Climate Anomaly (950−1250) that were in some regions as warm as in the late 20th century. These intervals did not occur as coherently across seasons and regions as the warming in the late 20th century (*high confidence*). {5.3.5, 5.5.1}

- It is *virtually certain* that globally the troposphere has warmed and the stratosphere has cooled since the mid-20th century. There is *medium confidence* in the rate of change and its vertical structure in the Northern Hemisphere extra-tropical troposphere and *low confidence* elsewhere. {2.4.4}

- Because of data insufficiency, *confidence* in precipitation change averaged over global land areas since 1901 is *low* prior to 1950 and *medium* afterwards. The incomplete records show mixed and non-significant long-term trends in global mean changes. Precipitation has increased in the mid-latitude land areas of the Northern Hemisphere since 1901 (*medium confidence* prior to 1950 and *high confidence* afterwards). {2.5.1}

- Changes in many extreme weather and climate events have been observed since about 1950 (see Table SPM.1). It is *very likely* that the number of cold days and nights has decreased and the number of warm days and nights has increased on the global scale. In some regions, it is *likely* that the frequency of heat waves has increased. There are *likely* more land regions where the number of heavy precipitation events has increased than where it has decreased. Regional trends vary, but confidence is highest for North America with *very likely* trends towards heavier precipitation events. {2.6.1, 2.6.2; FAQ 2.2}

[3] In the WGI contribution to the AR5, uncertainty is quantified using 90% uncertainty intervals unless otherwise stated. The 90% uncertainty interval, reported in square brackets, is expected to have a 90% likelihood of covering the value that is being estimated. The upper endpoint of the uncertainty interval has a 95% likelihood of exceeding the value that is being estimated and the lower endpoint has a 95% likelihood of being less than that value. A best estimate of that value is also given where available. Uncertainty intervals are not necessarily symmetric about the corresponding best estimate.

[INSERT TABLE SPM.1 HERE]
Table SPM.1: Extreme weather and climate events: Global-scale assessment of recent observed changes, human contribution to the changes, and projected further changes for the early (2016–2035) and late (2081–2100) 21st century. Bold indicates where the AR5 (black) provides a revised* global-scale assessment from the SREX (blue) or AR4 (red). Projections for early 21st century were not provided in previous assessment reports. Projections in the AR5 are relative to the reference period of 1986–2005, and use the new RCP scenarios.

Ocean

It is *virtually certain* that the upper ocean (0−700 m) has warmed from 1971 to 2010, and *likely* between the 1870s and 1971. Since the 1990s, when sufficient deep-ocean observations have become available to allow an assessment, the deep ocean below 3000 m depth has *likely* warmed. {3.2; Box 3.1; FAQ 3.1}

- The ocean warming is largest near the surface and exceeds 0.1°C per decade in the upper 75 m over the period 1971−2010. Since AR4, instrumental biases in upper-ocean temperature records have been identified and mitigated, reducing spurious decadal variability that was most prominent in the 1970s and 1980s. The warming decreases with depth and extends to 2000 m. From 1992 to 2005, no significant temperature trends were observed between 2000 and 3000 m depth. Warming below 3000 m is largest near the sources of deep and bottom water in the North Atlantic and the Southern Ocean. {3.2.4; FAQ 3.1}

- It is *virtually certain* that upper ocean (0–700 m) heat content increased during the relatively well-sampled 40-year period from 1971 to 2010. The increase estimated from a linear trend is 17 [15 to 19] $\cdot 10^{22}$ J. According to some estimates, ocean heat content from 0–700 m increased more slowly during 2003–2010 than over the previous decade, while ocean heat uptake from 700–2000 m *likely* continued unabated (Figure SPM.2c). {3.2.3, 3.2.4; Box 9.2}

- Ocean warming dominates the change in energy stored in the climate system. Warming of the ocean accounts for about 93% of this change between 1971 and 2010. Most of the net energy increase (about 64%) is stored in the ocean shallower than 700 m. {3.2.3; Box 3.1}

- Regional trends in ocean salinity provide indirect evidence that the pattern of evaporation minus precipitation over the oceans has been enhanced since the 1950s (*medium confidence*). It is *very likely* that regions of high salinity where evaporation dominates have become more saline, while regions of low salinity where rainfall dominates have become fresher. {2.5, 3.3.2−3.3.4; 3.5, 3.21; FAQ 3.3}

Cryosphere

There is stronger evidence that the ice sheets and glaciers worldwide are losing mass and sea ice cover is decreasing in the Arctic, while the Antarctic sea ice cover shows a small increase. This evidence is based on more comprehensive and improved observations extending over longer time periods. Northern Hemisphere spring snow cover is decreasing and permafrost is thawing. {4.2–4.7}

- There is *very high confidence* that glaciers have continued to shrink and lose mass world-wide, with very few exceptions. The rate of mass loss, excluding glaciers on the periphery of the ice sheets, was *very likely* 226 [91 to 361] Gt yr^{-1} over the period 1971−2009, and *very likely* 275 [140 to 410] Gt yr^{-1} over the period 1993−2009.[4] {4.3.3; Figures 4.9–4.12; Table 4.5; FAQ 4.1}

[4] 100 Gt yr^{-1} of ice loss corresponds to about 0.28 mm yr^{-1} of sea level equivalent.

- There is *very high confidence* that the Greenland Ice Sheet has lost mass during the last two decades. The average rate of mass loss has *very likely* increased from 34 [−6 to 74] Gt yr^{-1} over the period 1992–2001 to 215 [157 to 274] Gt yr^{-1} over the period 2002–2011. {4.4.2, 4.4.3}

- There is *high confidence* that the Antarctic Ice Sheet has lost mass during the last two decades. The average rate of mass loss *likely* increased from 30 [−37 to 97] Gt yr^{-1} over the period 1992–2001 to 147 [72 to 221] Gt yr^{-1} over the period 2002–2011. There is *very high confidence* that these losses are mainly from the northern Antarctic Peninsula and the Amundsen Sea sector of West Antarctica. {4.4.2, 4.4.3}

[INSERT FIGURE SPM.2 HERE]
Figure SPM.2: Multiple observed indicators of a changing global climate: (a) Northern Hemisphere March-April average snow cover extent, (b) Arctic July-August-September average sea ice extent, (c) change in global mean upper ocean heat content normalized to 2006−2010, and relative to the mean of all datasets for 1971, (d) global mean sea level relative to the 1900–1905 mean of the longest running dataset, and with all datasets aligned to have the same value in 1993, the first year of altimetry data. All time-series (coloured lines) show annual values, and where assessed, uncertainties are indicated by different shades of grey. See Chapter 2 Supplementary Material 2.SM.5 for a listing of the datasets. {Figures 3.2, 3.13, 4.19, and 4.3; FAQ 2.1, Figure 2; Figure TS.1}

- The annual mean Arctic sea ice extent decreased over the period 1979–2012 with a rate that was *very likely* in the range of 3.5 to 4.1% per decade. The extent of multi-year sea ice *very likely* decreased by over 11% per decade. The average decrease in decadal mean extent of Arctic sea ice has been most rapid in summer and autumn (*high confidence*), but the extent has decreased in every season, and in every successive decade since 1979 (*high confidence*) (Figure SPM.2b). There is *medium confidence* from reconstructions that summer sea ice retreat and increase in sea surface temperatures in the Arctic over the past three decades are anomalous in the perspective of at least the last 2,000 years. {4.2.2, 5.5.2}

- It is *very likely* that the annual mean Antarctic sea ice extent increased at a rate of in the range of 1.2 to 1.8% per decade between 1979 and 2012. There is *high confidence* that there are strong regional differences in this annual rate, with some regions increasing in extent and some decreasing. {4.2.3; FAQ 4.2}

- There is *very high confidence* that Northern Hemisphere snow cover extent has decreased since the mid-20th century, especially in spring (see Figure SPM.2a). Averaged March and April Northern Hemisphere snow cover extent decreased 1.6 [0.8 to 2.4] % per decade over the 1967−2012 period. During this period, snow cover extent in the Northern Hemisphere did not show a statistically significant increase in any months. {4.5.2}

- There is *high confidence* that permafrost temperatures have increased in most regions since the early 1980s, although the rate of increase has varied regionally. The temperature increase for colder permafrost was generally greater than for warmer permafrost (*high confidence*). A significant reduction in permafrost thickness and areal extent has occurred in the Russian European North over the period 1975−2005 (*medium confidence*). {4.7.2}

Sea Level

Global mean sea level has risen by 0.19 [0.17 to 0.21] m over the period 1901−2010 estimated from a linear trend , based on tide gauge records and additionally on satellite data since 1993 (see Figure SPM.2d). Based on proxy and instrumental data, it is *virtually certain* that the rate of global mean sea level rise has accelerated during the last two centuries. The current centennial rate of global mean sea level rise is unusually high in the context of centennial-scale variations over the last two millennia (*medium confidence*). {3.7, 5.6, 13.2}

- It is *very likely* that the mean rate of global averaged sea level rise was 1.7 [1.5 to 1.9] mm yr^{-1} between 1901 and 2010 and 3.2 [2.8 to 3.6] mm yr^{-1} between 1993 and 2010. Tide-gauge and satellite altimeter data are consistent regarding the higher rate of the latter period. It is *likely* that similarly high rates occurred between 1920 and 1950. {3.7.2, 3.7.3}

- There is *very high confidence* that the maximum global mean sea level was at least 5 m higher than present and *high confidence* that it did not exceed 10 m above present during the last interglacial period (129,000 to 116,000 years ago), when the global mean surface temperature was, with *medium confidence*, not more than 2°C warmer than pre-industrial. This sea level is higher than reported in AR4 owing to more widespread and comprehensive paleoclimate reconstructions. During the last interglacial period, the Greenland ice sheet *very likely* contributed between 1.4 and 4.3 m sea level equivalent, implying with *medium confidence* a contribution from the Antarctic ice sheet to the global mean sea level. {5.3.4, 5.6.2}

Carbon and Other Biogeochemical Quantities

The concentration of CO_2 in the atmosphere has increased by more than 20% since 1958 when systematic atmospheric measurements began (see Figure SPM.3), and by about 40% since 1750. The increase is a result of human activity, virtually all due to burning of fossil fuels and deforestation, and a small contribution from cement production. Present-day concentrations of CO_2, methane (CH_4), and nitrous oxide (N_2O) substantially exceed the range of concentrations recorded in ice cores during the past 800,000 years. The mean rates of CO_2, CH_4 and N_2O rise in atmospheric concentrations over the past century are, with *very high confidence*, unprecedented in the last 22,000 years. {2.2, 5.2, 6.2, 6.3}

- The concentrations of the greenhouse gases CO_2, CH_4, N_2O have all increased since 1750. There is *very high confidence* that in 2011 they exceeded the preindustrial levels by about 40%, 150%, and 20%, respectively. {2.2.1, 6.1, 6.2}

- By 2011, CO_2 emissions from fossil fuel combustion and cement production have released 365 [335 to 395] PgC (see [5]) to the atmosphere, while deforestation and other land use change are estimated to have released 180 [100 to 260] PgC since 1750. {6.3.1}

- While the total anthropogenic CO_2 emissions from 1750 to 2011 is 545 [460 to 630] PgC, 240 [230 to 250] PgC have accumulated in the atmosphere. This has increased the atmospheric CO_2 concentration from 278 [273 to 283] ppm (see [6]) in 1750 to 390.5 ppm in 2011 (see Figure SPM.3). {2.2.1, 6.3}

- The amount of anthropogenic carbon taken up by the global ocean is estimated at 155 [125 to 185] PgC in 2011. Natural terrestrial ecosystems not affected by land use change are estimated to have accumulated 150 [60 to 240] PgC since 1750, which is an amount similar to the carbon released from deforestation and other land use change. {3.8.1, 6.3}

- It is *very likely* that oceanic uptake of anthropogenic CO_2 results in acidification of the ocean. The pH (see [7]) of seawater has decreased by 0.1 since the beginning of the industrial era, corresponding to a 26% increase in hydrogen ion concentration. {3.8.2; Box 3.2; FAQ 3.2}

[5] 1 Petagram of carbon = 1 PgC = 10^{15} grams of carbon = 1 Gigatonne of carbon = 1 GtC. This corresponds to 3.67 $GtCO_2$.

[6] ppm (parts per million) or ppb (parts per billion, 1 billion = 1,000 million) is the ratio of the number of gas molecules to the total number of molecules of dry air. For example, 300 ppm means 300 molecules of a gas per million molecules of dry air.

[7] pH is a measure of acidity: a decrease in pH value means an increase in acidity, i.e., acidification.

[INSERT FIGURE SPM.3 HERE]
Figure SPM.3: Multiple observed indicators of a changing global carbon cycle. Measurements of atmospheric concentrations of carbon dioxide (CO_2) are from Mauna Loa and South Pole since 1958. Measurements of partial pressure of CO_2 at the ocean surface are shown from three stations from the Atlantic (29°10′N, 15°30′W – dark blue/dark green; 31°40′N, 64°10′W – blue/green) and the Pacific Oceans (22°45′N, 158°00′W − light blue/light green), along with the measurement of in situ pH, a measure of the acidity of ocean water (smaller pH means greater acidity). Full details of the datasets shown here are provided in the underlying report. {Figures 2.1 and 3.17; Figure TS.5}

Drivers of Climate Change

Natural and anthropogenic substances and processes that cause imbalances in the Earth's energy budget are drivers of climate change. Radiative forcing [8] (RF) quantifies the change in energy fluxes caused by changes in these drivers. All RF values are for the industrial era, defined here as 1750 to 2011, unless otherwise indicated. Positive RF leads to a warming, negative RF to a cooling. RF is estimated based on in-situ and remote observations, properties of greenhouse gases and aerosols, and calculations using numerical models representing observed processes. RF of anthropogenic substances can be reported based on emissions or atmospheric concentration changes. In this Summary for Policymakers, RF values are based on emissions, which provide a more direct link to human activities.

Total anthropogenic radiative forcing is positive, and has led to a net uptake of energy by the climate system. The increase in the atmospheric concentration of CO_2 since 1750 makes the largest contribution to net radiative forcing, and has also made the largest contribution to the increased anthropogenic forcing in every decade since the 1960s. Forcings due to the emission of aerosols and their interactions with clouds continue to contribute the largest uncertainty to estimates and interpretations of the Earth's changing energy budget. Changes in total solar irradiance and volcanic forcing contribute only a small fraction to the net radiative forcing during the industrial era (see Figure SPM.4). {Box 3.1, 7.5, 8.4, 8.5}

[INSERT FIGURE SPM.4 HERE]
Figure SPM.4: Radiative forcing estimates with respect to 1750 and uncertainties for the main drivers of climate change. Values are global average radiative forcing (RF, see [8]) partitioned according to the emitted compounds or processes that result in a combination of drivers. The best estimates of the net radiative forcing is shown as a black diamond with corresponding uncertainty intervals; the numerical values are provided on the right of the figure, together with the confidence level (VH – *very high*, H – *high*, M – *medium*, L – *low*, VL – *very low*). For halocarbons, confidence is H for ozone, and VH for CFCs and HCFCs. For aerosols, confidence is H for total aerosols, and M for individual aerosol components. Aerosol forcing other than cloud adjustments is the −0.27 W m^{-2} shown in the bar above and the −0.04 W m^{-2} from the nitrate response to NO_x emissions (which is equal to the −0.35 W m^{-2} due to aerosol-radiation interactions plus +0.04 W m^{-2} due to black carbon on snow), while the cloud adjustment term includes a response of −0.1 W m^{-2} due to aerosol-radiation interactions which is attributable to black carbon and −0.45 W m^{-2} that has not been attributed to individual components. Small forcings due to contrails, volcanoes, HFCs, PFCs and SF_6 are not shown. Total anthropogenic radiative forcing is provided for three different years with respect to 1750. {Figures 8.16 and 8.18; Figures TS.6 and TS.7}

[8] The strength of drivers is quantified as *Radiative Forcing* (RF) in units Watts per square metre (W m^{-2}) as in previous IPCC assessments. RF is the anomalous energy flux caused by a driver. In the traditional RF concept employed in previous IPCC reports all surface and tropospheric conditions are kept fixed. In this report, in calculations of RF for well-mixed greenhouse gases and aerosols, physical variables, except for the ocean and sea ice, are allowed to respond to perturbations with rapid adjustments. This change reflects the scientific progress from previous assessments and results in a better indication of the eventual temperature response for these drivers. For all other drivers, these adjustments are assumed to be small, and thus the traditional RF is taken as the best estimate of forcing.

- The total anthropogenic RF since 1750 is 2.3 [1.1 to 3.3] W m^{-2} (see Figure SPM.4), and it has increased more rapidly since 1970 than during prior decades. The total anthropogenic RF estimate for 2011 is 44% higher compared to the estimate reported in AR4 for the year 2005. This is due in about equal parts to reductions in estimates of the forcing resulting from aerosols and continued growth in most greenhouse gas concentrations. {8.5.1}

- The RF from changes in concentrations of well-mixed greenhouse gases (CO_2, CH_4, N_2O, and Halocarbons) since 1750 is 2.83 [2.26 to 3.40] W m^{-2}. {8.3.2}

- Emissions of CO_2 alone have caused an RF of 1.68 [1.33 to 2.03] W m^{-2} (see Figure SPM.4). Including emissions from other carbon-containing sources, which also contributed to the increase in CO_2 concentrations, yield an RF of 1.82 [1.46 to 2.18] W m^{-2}. {8.3.2, 8.5.1}

- Emissions of CH_4 alone have caused an RF of 0.97 [0.74 to 1.20] W m^{-2}. This is *very likely* much larger than the concentration-based estimate of 0.48 [0.38 to 0.58] Wm^{-2} (unchanged from AR4). This difference in estimates is caused by concentration changes in ozone and stratospheric water vapour due to CH_4 emissions and other emissions indirectly affecting CH_4 (see Figure SPM.4). {8.3.2, 8.3.3, 8.5.1; FAQ 8.2}

- Emissions of ozone-depleting halocarbons are *very likely* to have caused a net positive RF as their own positive RF has outweighed the negative RF from the stratospheric ozone depletion that they have induced (see Figure SPM.4). {8.3.3, 8.5.1; FAQ 8.2}

- Emissions of short-lived gases contribute substantially to radiative forcing. Emissions of carbon monoxide are *virtually certain* to have induced a positive RF, while emissions of NO_x are *likely* to have induced a net negative RF (see Figure SPM.4). {8.3.3, 8.5.1; FAQ 8.2}

- The RF of the total aerosol effect is –0.9 [–1.9 to −0.1] W m^{-2} (*medium confidence*), and results from a negative forcing from most aerosols and a positive contribution from black carbon absorption of solar radiation. While the uncertainty in the aerosol contribution dominates the overall uncertainty in total RF over the industrial era, there is *high confidence* that aerosols have offset a substantial portion of global mean forcing from well-mixed greenhouse gases. {2.2.3, 2.3.3, 7.5.1, 7.5.2, 8.3.4, 8.5.1}

- The forcing from stratospheric volcanic aerosols can have a large impact on the climate for some years after volcanic eruptions. Several small eruptions have caused an RF for the years 2008−2011 of −0.10 [–0.13 to –0.07] W m^{-2}, approximately double the 1999−2002 volcanic aerosol RF. {8.4.2}

- The best estimate of RF due to changes in total solar irradiance over the industrial era is 0.05 [0.00 to 0.10] W m^{-2} (see Figure SPM.4). Satellite observations of total solar irradiance changes from 1978 to 2011 indicate that the last solar minimum was lower than the previous two, resulting in a *likely* RF change of –0.04 [–0.08 to 0.00] W m^{-2} between the most recent (2008) minimum and the 1985 minimum. {8.4.1}

Understanding the Climate System and its Recent Changes

Understanding of the climate system results from combining observations, theoretical studies of feedback processes, and model simulations. Compared to AR4, more detailed observations and improved climate models now enable the attribution of detected changes to human influences in more climate system components.

Evaluation of Climate Models

Climate models have continued to be improved since the AR4, and many models have been extended into Earth System Models by including a representation of the carbon cycle. There is *very high confidence* that climate models reproduce the observed large-scale patterns and multi-decadal trends in surface temperature, especially since the mid-20th century. Confidence is lower on sub-continental and smaller spatial scales. Precipitation and sea ice cover are not simulated as well as surface temperature, but improvements have occurred since the AR4. {9.1, 9.4, 9.6, 9.8; Box 9.1; Box 9.2}

- There is *very high confidence* that models reproduce the more rapid warming in the second half of the 20th century, and the cooling immediately following large volcanic eruptions. Models do not generally reproduce the observed reduction in surface warming trend over the last 10–15 years. There is *medium confidence* that this difference between models and observations is to a substantial degree caused by unpredictable climate variability, with possible contributions from inadequacies in the solar, volcanic, and aerosol forcings used by the models and, in some models, from too strong a response to increasing greenhouse-gas forcing. {9.4.1, 10.3.1, 11.3.2; Box 9.2}

- There has been some improvement in the simulation of large-scale patterns of precipitation since the AR4. At regional scales, precipitation is not simulated as well, and the assessment remains difficult owing to observational uncertainties. {9.4.1, 9.6.1}

- Climate models now include more cloud and aerosol processes, and their interactions, than at the time of the AR4, but there remains *low confidence* in the representation and quantification of these processes in models. {7.3, 7.4, 7.5.2, 7.6.4, 9.4.1}

- There is robust evidence that the downward trend in Arctic summer sea ice extent since 1979 is now better simulated than at the time of the AR4, with about one-quarter of the models showing a trend as large as, or larger than, the trend in the observations. Most models simulate a small decreasing trend in Antarctic sea ice extent, albeit with large inter-model spread, in contrast to the small increasing trend in observations. {9.4.3}

- Many models reproduce the observed changes in upper-ocean heat content from 1960 to present, with the multi-model mean time series falling within the range of the available observational estimates for most of the period. {9.4.2}

- In the majority of Earth System Models the simulated global land and ocean carbon sinks over the latter part of the 20th century are within the range of observational estimates. However, models systematically underestimate the Northern Hemisphere land sink derived from atmospheric observations. {9.4.5}

Quantification of Climate System Responses

Independent estimates of radiative forcing, observed heat storage and surface warming combine to give an estimated energy budget for the Earth that is consistent with the assessed *likely* range of the equilibrium climate sensitivity to within assessed uncertainties. This ability to balance the Earth's energy budget over recent decades provides *high confidence* in the understanding of anthropogenic climate change. {Box 13.1}

- The net feedback from combined changes in amount and distribution of water vapour in the atmosphere is *extremely likely* positive and therefore amplifies changes in climate. The sign of the net radiative feedback due to all cloud types is *likely* positive. Uncertainty in the sign and magnitude of the cloud feedback is due primarily to continuing uncertainty in the impact of warming on low clouds. {7.2.4, 7.2.5, 7.2.6}

- The equilibrium climate sensitivity (ECS) quantifies the response of the climate system to constant radiative forcing. It is defined as change in global mean surface temperature at equilibrium that is caused by a doubling of the atmospheric CO_2 concentration. ECS is *likely* in the range 1.5°C to 4.5°C (*high confidence*), *extremely unlikely* less than 1°C (*high confidence*), and *very unlikely* greater than 6°C (*medium confidence*). The lower limit of the assessed *likely* range is thus less than the 2°C in the AR4, reflecting the evidence from new studies of observed temperature change using the extended records in atmosphere and ocean. {Box 12.2}

- The transient climate response (TCR) quantifies the response of the climate system to an increasing radiative forcing on a decadal to century timescale. It is defined as the change in global mean surface temperature at the time when the atmospheric CO_2 concentration has doubled in a scenario of concentration increasing at 1% per year. TCR is *likely* in the range of 1.0°C to 2.5°C (*high confidence*) and *extremely unlikely* greater than 3°C. {Box 12.2}

- The transient climate response to cumulative carbon emissions (TCRE) is the global mean surface temperature change per 1000 PgC emitted to the atmosphere. TCRE is *likely* in the range of 0.8°C to 2.5°C per 1000 PgC and applies for cumulative emissions up to about 2000 PgC until the time temperatures peak (see Figure SPM.9). {12.5.4; Box 12.2}

Detection and Attribution of Climate Change

It is *extremely likely* that human influence on climate caused more than half of the observed increase in global average surface temperature from 1951−2010. There is *high confidence* that this has warmed the ocean, melted snow and ice, raised global mean sea level, and changed some climate extremes, in the second half of the 20th century (see Figure SPM.5 and Table SPM.1). {10.3–10.6, 10.9}

[INSERT FIGURE SPM.5 HERE]
Figure SPM.5: Comparison of observed and simulated climate change based on time-series of three large-scale indicators in the atmosphere, the cryosphere and the ocean: continental land surface air temperatures (yellow panels), Arctic and Antarctic sea ice (white panels), ocean heat uptake in the major ocean basins (blue panels). Global average changes are also given. All time-series are decadal averages, plotted at the centre of the decade. For temperature panels, observations are dashed lines if the spatial coverage of areas being examined is below 50%. For ocean heat content and sea ice panels the solid line is where the coverage of data is good and higher in quality, and the dashed line is where the data coverage is only adequate, and thus, uncertainty is larger. Model results shown are CMIP5 multi-model means and ensemble ranges, with shaded bands indicating the 5 to 95% confidence intervals[9]. See Chapter 10, Supplementary Material 10.SM.1 for datasets and methods used. {Figure 10.21; Figure TS.12}

- The observed warming since 1951 can be attributed to the different natural and anthropogenic drivers and their contributions can now be quantified. Greenhouse gases contributed a global mean surface warming *likely* to be in the range of 0.5°C to 1.3 °C over the period 1951−2010, with the contributions from other anthropogenic forcings, including the cooling effect of aerosols, *likely* to be in the range of −0.6°C to 0.1 °C. The contributions from natural forcings are *likely* to be in the range of −0.1°C to 0.1 °C, and from internal variability *likely* to be in the range of −0.1°C to 0.1°C. Together these assessed contributions are consistent with the observed warming of approximately 0.6°C over this period. {10.3.1}

[9] For surface temperature, the blue shaded band is based on 52 simulations from 17 climate models using only natural forcings, while the red shaded band is based on 147 simulations from 44 climate models using natural and anthropogenic forcings. For ocean heat content, 10 simulations from 10 models, and 13 simulations from 13 models were used respectively. For sea ice extent, a subset of models are considered that simulated the mean and seasonal cycle of the sea ice extent within 20% of the observed sea-ice climatology for the period 1981–2005 (Arctic: 24 simulations from 11 models for both red and blue shaded bands, Antarctic: 21 simulations from 6 models for both red and blue shaded bands).

- The observed reduction in warming trend over the period 1998–2012 as compared to the period 1951–2012, is due in roughly equal measure to a cooling contribution from internal variability and a reduced trend in radiative forcing (*medium confidence*). The reduced trend in radiative forcing is primarily due to volcanic eruptions and the downward phase of the current solar cycle. However, there is *low confidence* in quantifying the role of changes in radiative forcing in causing this reduced warming trend. {Box 9.2; 10.3.1; Box 10.2}

- Over every continental region except Antarctica, anthropogenic forcings have *likely* made a substantial contribution to surface temperature increases since the mid-20th century (see Figure SPM.5). For Antarctica, large observational uncertainties result in *low confidence* that anthropogenic forcings have contributed to the observed warming averaged over available stations. {2.4.1, 10.3.1}

- It is *very likely* that anthropogenic forcings have made a substantial contribution to global upper ocean heat content (above 700 m) observed since the 1970s (see Figure SPM.5). Attribution of changes in regional upper ocean heat content is less certain. {3.2.3, 10.4.1}

- It is *likely* that anthropogenic influences have affected the global water cycle and its patterns since 1960. This assessment is based on the systematic changes observed, detected and attributed in terrestrial precipitation, atmospheric humidity, and oceanic surface salinity distributions influenced by precipitation and evaporation, the consistency of the evidence from both the atmosphere and ocean, and physical understanding. {2.5, 3.3.2, 7.6, 10.3.2, 10.4.2}

- Anthropogenic influences have *very likely* contributed to Arctic sea ice loss since 1979. There is *low confidence* in the scientific understanding of the small observed increase in Antarctic sea ice extent due to the incomplete and competing scientific explanations for the causes of change and *low confidence* in estimates of internal variability in that region. {10.5.1}

- Anthropogenic influences *likely* contributed to the retreat of glaciers since the 1960s and to the increased surface mass loss of the Greenland ice sheet since 1990. Due to a low level of scientific understanding there is *low confidence* in attributing the causes of the observed loss of mass from the Antarctic ice sheet over the past two decades. {4.3.3, 10.5.2}

- It is *likely* that there has been an anthropogenic component to observed reductions in Northern Hemisphere snow cover since 1970. {10.5.3}

- Since the early 1970s, glacier mass loss and ocean thermal expansion from warming together explain about 75% of the observed global mean sea level rise. Over the period 1993−2010, global mean sea level rise is consistent with the sum of the observed contributions from ocean thermal expansion due to warming, and from changes in mass of glaciers, ice sheets and land water storage. {13.3.6}

- Based on the *high confidence* in an anthropogenic influence on three of the main contributors to sea level, that is thermal expansion, glacier mass loss, and Greenland ice sheet surface mass loss, it is *very likely* that there is a substantial anthropogenic contribution to the global mean sea level rise since the 1970s. {10.4.1, 10.4.3, 10.5.2, 13.3.6}

- There is *high confidence* that changes in total solar irradiance have not contributed to global warming over the period 1986 to 2008, when direct satellite measurements of total solar irradiance were available. There is *medium confidence* that the 11-year cycle of solar variability influences decadal climate fluctuations in some regions through other amplifying mechanisms. {10.3.1; Box 10.2}

- Cosmic rays enhance new particle formation in the free troposphere, but the effect on the concentration of cloud condensation nuclei is too weak to have any detectable climatic influence during a solar cycle or over the last century (*medium evidence, high agreement*). No robust association between changes in cosmic rays and cloudiness has been identified. {7.4.6}

Future Global and Regional Climate Change

Projections of changes in the climate system are made using a hierarchy of climate models ranging from simple climate models, to models of intermediate complexity, to comprehensive climate models, and Earth System Models. These models simulate changes based on a set of scenarios of anthropogenic forcings. A new set of scenarios, the Representative Concentration Pathways (RCPs), was used for the new climate model simulations carried out under the framework of the Coupled Model Intercomparison Project Phase 5 (CMIP5) of the World Climate Research Programme (see Box SPM.1). A large number of comprehensive climate models and Earth System Models have participated in CMIP5, whose results form the core of the climate system projections. Projections in this Summary for Policymakers are given relative to 1986–2005, unless otherwise stated[10].

Continued emissions of greenhouse gases would cause further warming. Emissions at or above current rates would induce changes in all components in the climate system, some of which would *very likely* be unprecedented in hundreds to thousands of years. Changes are projected to occur in all regions of the globe, and include changes in land and ocean, in the water cycle, in the cryosphere, in sea level, in some extreme events and in ocean acidification. Many of these changes would persist for many centuries. Limiting climate change would require substantial and sustained reductions of CO_2 emissions. {Chapters 5, 6, 11, 12, 13, 14}

- Projections of many quantities for the next few decades show further changes that are similar in patterns to those already observed. They provide an indication of changes that are projected later in the 21st century. For some quantities, natural variability continues to be larger than the forced changes, particularly at the regional scale. By about mid-21st century the magnitudes of the projected changes are substantially affected by the choice of emissions scenario (Box SPM.1). {11.3.1, 11.3.2, 11.3.6; Box 11.1; FAQ 11.1; Annex I}

[INSERT BOX SPM.1 HERE]
Box SPM.1: Representative Concentration Pathways (RCPs)

- Projected climate change based on RCPs is similar to AR4 after accounting for scenario differences. The overall spread of projections for the high RCPs is narrower than for comparable scenarios used in AR4 because in contrast to the SRES emission scenarios used in AR4, the RCPs used in AR5 are defined as concentration pathways and thus carbon cycle uncertainties affecting atmospheric CO_2 concentrations are not considered in the concentration driven CMIP5 simulations. Simulated patterns of climate change in the CMIP5 models are very similar to CMIP3. {11.3.6, 12.3, 12.4, 12.4.9}

[INSERT FIGURE SPM.6 HERE]
Figure SPM.6: CMIP5 multi-model simulated time series from 1950 to 2100 for (a), change in global annual mean surface temperature relative to 1986–2005, see Table SPM.2 and footnote 9 for other reference periods. (b), Northern Hemisphere sea ice extent in September (5 year running mean), and (c), global mean ocean surface pH. Time series of projections and a measure of uncertainty (shading, minimum-maximum range) are shown for scenarios RCP2.6 (blue) and RCP8.5 (red). Black (grey shading) is the modelled historical evolution using historical reconstructed forcings. The mean and associated uncertainties averaged over 2081−2100 are given for all RCP scenarios as colored vertical bars. The numbers of CMIP5 models used to calculate the multi-model mean is indicated. For sea ice extent (b), the projected mean and uncertainty (minimum-maximum range) of the subset of models that most closely reproduce the climatological mean state and 1979–2012 trend of the Arctic sea ice is given. For completeness, the CMIP5 multi-model mean is indicated with dashed lines. {Figures 6.28, 12.5, and 12.28–12.31; Figures TS.15, TS.17, and TS.20}

[10] Using HadCRUT4 and its uncertainty estimate (5−95% confidence interval), the observed warming to the reference period 1986−2005 used for projections is 0.61 [0.55 to 0.67] °C for 1850−1900, 0.30 [0.27 to 0.33] °C for 1961−1990, and 0.11 [0.09 to 0.13] °C for 1980−1999. {2.4.3}

[INSERT FIGURE SPM.7 HERE]
Figure SPM.7: Maps of CMIP5 multi-model mean results for the scenarios RCP2.6 and RCP8.5 in 2081–2100 of (a), surface temperature change, (b), average percent change in mean precipitation, (c), Northern Hemisphere September sea ice extent, and (d) change in ocean surface pH. Changes in panels (a), (b) and (d) are shown relative to 1986–2005. The number of CMIP5 models to calculate the multi-model mean is indicated in the upper right corner of each panel. For panels (a) and (b), hatching indicates regions where the multi model mean is less than one standard deviation of internal variability. Stippling indicates regions where the multi model mean is greater than two standard deviations of internal variability and where 90% of models agree on the sign of change (see Box 12.1). In panel (c), the lines are the modeled means for 1986−2005; the filled areas are for the end of the century. The CMIP5 multi-model mean is given in white color, the projected mean sea ice extent of a subset of models that most closely reproduce the climatological mean state and 1979–2012 trend of the Arctic sea ice cover is given in grey color. {Figures 6.28, 12.11, 12.22, and 12.29;Figures TS.15, TS.16, TS.17, and TS.20}

[INSERT TABLE SPM.2 HERE]
Table SPM.2: Projected change in global mean surface air temperature and global mean sea level rise for the mid- and late 21st century. {12.4.1; Table 12.2, Table 13.5}

Atmosphere: Temperature

The total anthropogenic emission of long-lived greenhouse gases largely determines the warming in the 21st century. Surface temperature change will not be regionally uniform, and there is *very high confidence* that long-term mean warming over land will be larger than over the ocean and that the Arctic region will warm most rapidly (see Figures SPM 6 and SPM.7). {12.3, 12.4; Box 5.1}

- The global mean surface temperature change for the period 2016–2035 will *likely* be in the range of 0.4°C to 1.0°C for the set of RCPs. This is based on an assessment of observationally-constrained projections and predictions initialized with observations (*medium confidence*). {11.3.2}

- Increase of global mean surface temperatures for 2081–2100 for the CO_2 concentration driven RCPs is projected to *likely* be in the ranges derived from the CMIP5 climate models, i.e., 0.3°C to 1.7°C (RCP2.6), 1.1°C to 2.6°C (RCP4.5), 1.4°C to 3.1°C (RCP6.0), 2.6°C to 4.8°C (RCP8.5) (see Figure SPM.6 and Table SPM.2). {12.4.1}

- With respect to preindustrial conditions, global temperatures averaged in the period 2081−2100 are projected to *likely* exceed 1.5°C above preindustrial for RCP4.5, RCP6.0 and RCP8.5 (*high confidence*) and are *likely* to exceed 2°C above preindustrial for RCP6.0 and RCP8.5 (*high confidence*). Temperature change above 2°C under RCP2.6 is *unlikely* (*medium confidence*). Warming above 4°C by 2081−2100 is *unlikely* in all RCPs (*high confidence*) except for RCP8.5 where it is *as likely as not* (*medium confidence*). {12.4.1}

- It is *virtually certain* that, in most places, there will be more hot and fewer cold temperature extremes on daily and seasonal timescales as global mean temperatures increase. It is *very likely* that heat waves will occur with a higher frequency and duration; however, occasional cold winter extremes will continue to occur. (Table SPM.1). {12.4.3}

Atmosphere: Water Cycle

There is *high confidence* that the contrast of seasonal mean precipitation between dry and wet regions will increase in a warmer climate over most of the globe in the 21st century, although there may be regional exceptions. Furthermore, there is *high confidence* that the contrast between wet and dry seasons will increase over most of the globe as temperatures increase. The high latitudes and the equatorial Pacific Ocean are *very likely* to experience more precipitation (see Figure SPM.7). {12.4}

- Projected changes in the water cycle over the next few decades show similar large-scale patterns to those towards the end of the century, but with smaller magnitude. In the next few decades projected changes at the regional-scale will be strongly influenced by internal variability. {11.3.2}

- In many mid-latitude and subtropical dry regions, mean precipitation will *likely* decrease, while in many mid-latitude wet regions, mean precipitation will *likely* increase by the end of this century under the RCP8.5 scenario (see Figure SPM.7). In a warmer world, extreme precipitation events over most of the mid-latitude land masses and over wet tropical regions will *very likely* be more intense and more frequent by the end of this century (see Table SPM.1) {7.6.2, 7.6.5, 12.4.5}

- Globally, it is *likely* that the area encompassed by monsoon systems will increase over the 21st century. Also, while monsoon circulation is *likely* to weaken, monsoon precipitation is *likely* to intensify. Monsoon onset dates are *likely* to become earlier or not to change much. Monsoon retreat dates will *very likely* be delayed, resulting in lengthening of the monsoon season. {14.2.1}

- The El Niño-Southern Oscillation (ENSO) will *very likely* remain the dominant mode of interannual variability in the tropical Pacific, with global influences in the 21st century. Due to changes in moisture availability, ENSO-related precipitation variability on regional scales will *likely* intensify. Natural modulations of the variance and spatial pattern of ENSO are large and thus *confidence* in any specific projected change for the 21st century remains *low*. {5.4, 14.4}

Atmosphere: Air Quality

- Background levels of surface ozone (O_3) on continental scales are projected to decrease over most regions as rising temperatures enhance global O_3 destruction (*high confidence*), but to increase with rising methane (*high confidence*). By 2100, surface ozone increases by about 8 ppb globally in the doubled-methane scenario (RCP8.5) relative to the stable-methane pathways. All else being equal, there is *medium confidence* that warmer temperatures are expected to trigger positive feedbacks in chemistry and local emissions, further enhancing pollution levels. {11.3.5; Annex II}

Ocean

The global ocean is projected to warm in all RCP scenarios. Due to the long time scales of heat transfer from the surface to depth, ocean warming will continue for centuries, even if greenhouse gas emissions are decreased or concentrations kept constant. {12.4}

- The strongest warming signal is projected for the surface in subtropical and tropical regions. At greater depth the warming will be most pronounced in the Southern Ocean. In some regions, ocean warming in the top few hundred meters is projected to exceed 0.5°C (RCP2.6) to 2.5°C (RCP8.5), and 0.3°C (RCP2.6) to 0.7°C (RCP8.5) at a depth of about 1 km by the end of the century. {12.4.7}

- It is *very likely* that the Atlantic Meridional Overturning Circulation (AMOC) will weaken over the 21st century by about 20 to 30% in the RCP4.5 scenario, and about 36 to 44% in the RCP8.5 scenario. It is *likely* that there will be some decline in the AMOC by 2050, but there will be some decades when the AMOC increases. {11.3.3, 12.4.7}

- It is *very unlikely* that the AMOC will undergo an abrupt transition or collapse in the 21st century for the scenarios considered. There is *low confidence* in assessing the evolution of the AMOC beyond the 21st century because of the limited number of analyses and equivocal results. A collapse beyond the 21st century for large sustained warming cannot be excluded. {12.5.5}

Cryosphere

It is *very likely* that the Arctic sea ice cover will continue to shrink and thin and that Northern Hemisphere snow cover will decrease during the 21st century as global temperature rises. It is *virtually certain* that near-surface permafrost extent at high northern latitudes will be reduced. Glacier volume is projected to decrease under all RCP scenarios. {12.4, 13.4}

- By the end of the century, year-round reductions in Arctic sea ice are projected from CMIP5 multi-model averages, with reductions in sea ice extent for 2081–2100 ranging from 43% for RCP2.6 to 94% for RCP8.5 in September and from 8% to 34% in February (*medium confidence*) (see Figures SPM.6 and SPM.7). {12.4.6}

- Based on an assessment of a subset of models that most closely reproduce the climatological mean state and 1979–2012 trend of the Arctic sea ice cover, a nearly ice-free Arctic Ocean[11] in September before mid-century is *likely* under RCP8.5 (*medium confidence*) (see Figures SPM.6 and SPM.7). {11.3.4, 12.4.6, 12.5.5}

- In the Antarctic, a decrease in sea ice extent and volume is projected with *low confidence* for the end of the 21st century as global mean surface temperature rises. {12.4.6}

- By 2100, 15 to 55% of the present glacier volume is eliminated under RCP2.6, and 35 to 85% under RCP8.5 (*medium confidence*). {13.4.2, 13.5.1}

- The area of Northern Hemisphere spring snow cover is projected to decrease by 7% for RCP2.6 and by 25% in RCP8.5. {12.4.6}

- By the end of the 21st century, diagnosed near-surface permafrost area is projected to decrease by between 37% (RCP2.6) to 81% (RCP8.5) (*medium confidence*). {12.4.6}

Sea Level

Global mean sea level will rise during the 21st century (see Figure SPM.8). Confidence in projections of global mean sea level rise has increased since the AR4 because of the improved agreement of process-based models with observations and physical understanding, and the inclusion of ice-sheet rapid dynamical changes. {13.3–13.5}

- It is *very likely* that the rate of global mean sea level rise during the 21st century will exceed the rate observed during 1971–2010 for all RCP scenarios, due to increased ocean warming and loss of mass of glaciers and ice sheets. {13.5.1, 13.5.3}

[INSERT FIGURE SPM.8 HERE]
Figure SPM.8: Projections of global mean sea level change over the 21st century relative to 1986−2005 from the combination of CMIP5 and process-based models, for the two emissions scenarios RCP2.6, and RCP8.5. The assessed *likely* range is shown as a shaded band. The assessed *likely* ranges for the mean over the period 2081−2100 for all RCP scenarios are given as coloured vertical bars, with the corresponding median value given as a horizontal line. Based on current understanding, only the collapse of marine-based sectors of the Antarctic ice sheet, if initiated, could cause global mean sea level to rise substantially above the *likely* range during the 21st century. However, there is *medium confidence* that this additional contribution would not exceed several tenths of a meter of sea level rise during the 21st century. {Table 13.5, Figures13.10 and 13.11; Figures TS.21 and TS.22}

[11] Conditions in the Arctic Ocean are referred to as ice-free when the sea ice extent is less than 10^6 km^2.

- Global mean sea level rise for 2081−2100 will *likely* be in the ranges of 0.26 to 0.54 m for RCP2.6, 0.32 to 0.62 m for RCP4.5, 0.33 to 0.62 m for RCP6.0, and 0.45 to 0.81 m for RCP8.5 (*medium confidence*). These ranges are derived from CMIP5 climate projections in combination with process-based models and literature assessment of glacier and ice sheet contributions. For RCP8.5 the rate of global mean sea level rise is 7 to 15 mm yr^{-1} during 2081−2100 and the range in year 2100 is 0.53 to 0.97 m. (see Figure SPM.8, Table SPM.2). {13.5.1, 13.5.3}

- The basis for higher projections of global mean sea level rise in the 21st century has been considered and it has been concluded that there is currently insufficient evidence to evaluate the probability of specific levels above the *likely* range. Based on current understanding, only the collapse of marine-based sectors of the Antarctic Ice Sheet, if initiated, could cause global mean sea level to rise substantially above the *likely* range during the 21st century. However, there is *medium confidence* that this additional contribution would not exceed several tenths of a meter of sea level rise during the 21st century. {13.4.4, 13.5.3}

- Many semi-empirical model projections of global mean sea level rise are higher than process-based model projections, but there is low agreement in semi-empirical model projections, and no consensus about their reliability. {13.5.2, 13.5.3}

- In all RCP scenarios, thermal expansion is the largest contribution to future global mean sea level rise, accounting for 30 to 55% of the total, with the second largest contribution coming from glaciers. There is *high confidence* that the increase in surface melting of the Greenland ice sheet will exceed the increase in snowfall, leading to a positive contribution from changes in surface mass balance to future sea level. There is *medium confidence* that snowfall on the Antarctic ice sheet will increase, while surface melting will remain small, resulting in a negative contribution to future sea level from changes in surface mass balance. Rapid changes in outflow from both ice sheets combined will *likely* make a contribution in the range of 0.03 to 0.20 m by 2081−2100. {13.3.3, 13.4.2−13.4.4, 13.5.1}

- By the end of the 21st century, it is *very likely* that sea level will rise in more than about 95% of the ocean area. About 70% of the coastlines worldwide are projected to experience sea level change within 20% of the global mean sea level change. In some coastal locations, past and current glacier and ice-sheet mass loss, tectonic processes, coastal processes, and local anthropogenic activity are also important contributors to changes in sea level relative to the land. {13.1.4, 13.6.5}

Carbon and Other Biogeochemical Cycles

In all RCPs, atmospheric CO_2 concentrations are higher in 2100 relative to present day as a result of a further increase of cumulative emissions of CO_2 to the atmosphere during the 21st century. Part of the CO_2 emitted to the atmosphere by human activity will continue to be taken up by the ocean. Future CO_2 uptake by the land is model and scenario dependent. It is *virtually certain* that the resulting storage of carbon by the ocean will increase ocean acidification. {6.4}

- With *very high confidence,* ocean carbon uptake of anthropogenic CO_2 emissions will continue under all four RCPs through to 2100, with higher uptake for higher concentration pathways. The future evolution of the land carbon uptake is much more uncertain, with a majority of models projecting a continued net carbon uptake under all RCPs, but with some models simulating a net loss of carbon by the land due to the combined effect of climate change and land use change. {6.4.3}

- Based on Earth System Models, there is *high confidence* that the feedback between climate and the carbon cycle is positive in the 21st century, i.e., climate change will partially offset land and ocean carbon sinks, leaving more of the emitted CO_2 in the atmosphere. A positive feedback between climate and the carbon cycle on century to millennial time scales is supported by paleoclimate observations and modelling. {6.2.3, 6.4.2}

- Earth System Models project a worldwide increase in ocean acidification for all RCP scenarios. The corresponding decrease in surface ocean pH by the end of 21st century is 0.065 (0.06 to 0.07)[12] for RCP2.6, 0.145 (0.14 to 0.15) for RCP4.5, 0.203 (0.20 to 0.21) for RCP6.0, and 0.31 (0.30 to 0.32) for RCP8.5 (see Figures SPM.6 and SPM.7). {6.4.4}

- Cumulative fossil fuel emissions for the 2012−2100 period compatible with the RCP atmospheric CO_2 concentrations, as derived from CMIP5 Earth System Models, are 270 (140 to 410)[12] PgC for RCP2.6 , 780 (595 to 1005) PgC for RCP4.5, 1060 (840 to 1250) PgC for RCP6.0, and 1685 (1415 to 1910) PgC for RCP8.5. For RCP2.6, an average emission reduction of 50% (range 14% to 96%) is required by 2050 relative to 1990 levels. It is about as *likely as not* that sustained globally net negative CO_2 emissions, i.e., net removal of CO_2 from the atmosphere, will be required to achieve the reductions in atmospheric CO_2 in this scenario by the end of the 21st century. {6.4.3}

- There is *low confidence* in projections of the magnitude of additional carbon emissions to the atmosphere through CO_2 or CH_4 release from thawing permafrost. The best estimate range for 2100 is 50 to more than 250 PgC for RCP8.5. {6.4.3}

Climate Stabilization, Climate Change Commitment and Irreversibility

The principal driver of long-term warming is total emissions of CO_2 and the two quantities are approximately linearly related (see Figure SPM.9). Therefore, for any given warming target, higher emissions in earlier decades imply lower emissions later. Many aspects of climate change will persist for many centuries even if emissions of greenhouse gases are stopped. This represents a substantial multi-century commitment created by past, present and future emissions of CO_2. {12.5}

[INSERT FIGURE SPM.9 HERE]

Figure SPM.9: Global mean temperature increase as a function of cumulative total global CO_2 emissions from various lines of evidence. Multi-model results from a hierarchy of climate-carbon cycle models for each RCP until 2100 shown with coloured lines and decadal means (dots). The decadal means for 2001−2010 (star), 2041−2050 (square) and 2091−2100, (diamond) are highlighted. Model results over the historical period (1860–2010) are indicated in black. The coloured plume illustrates the multi-model spread over the four RCP scenarios and fades with the decreasing number of available models. The multi-model mean and range simulated by CMIP5 models, forced by a CO_2 increase of 1% per year, is given by the thin black line and dark grey area. The light grey wedge represents this report's assessment of the transient climate response to emissions (TCRE) from CO_2 only. All values are given relative to the 1861−1880 base period. The horizontal brown bar and solid black line at the bottom-left illustrate the assessment of total cumulative carbon emissions until 2011 with associated uncertainties. All time-series are represented by connecting decadal averages to illustrate the long-term trends. {Figure 12.45; TFE.8, Figure 1}

- Based on the assessment of TCRE, cumulative CO_2 emissions from all anthropogenic sources would need to be limited to about 1000 PgC since the beginning of the industrial era, if the warming caused by anthropogenic CO_2 emissions alone is limited to be *likely* less than 2°C relative to pre-industrial. About half of this budget, estimated in the range of 460 to 630 PgC, was already emitted by 2011. Accounting for the projected warming effect of non-CO_2 forcings, a possible release of greenhouse gases from permafrost or methane hydrates, or requiring a higher likelihood of temperatures remaining below 2°C, all imply a substantially lower budget. (see Figure SPM.9). {12.5.4}

- It is *very likely* that more than 20% of emitted CO_2 will remain in the atmosphere longer than 1,000 years after anthropogenic emissions have stopped. CO_2 induced warming is projected to remain approximately constant for many centuries following a complete cessation of emissions. A large fraction of climate change is thus irreversible on a human time scale, except if net anthropogenic CO_2 emissions were strongly negative over a sustained period. {Box 6.2; 12.5.5}

[12] The brackets ( ) in this paragraph indicate a CMIP5 model spread.

- It is *virtually certain* that global mean sea level rise will continue beyond 2100, with sea level rise due to thermal expansion to continue for many centuries. The few available model results indicate global mean sea level rise by 2300 to be less than 1 m for a radiative forcing that corresponds to CO_2 concentrations that peak and decline and remain below 500 ppm, but 1 to 3 m for a radiative forcing that corresponds to a CO_2 concentration that is above 700 ppm (*medium confidence*). {13.5.4}

- Larger sea level rise could result from sustained mass loss by ice sheets, and some part of the mass loss might be irreversible. The available evidence indicates that sustained warming greater than a certain threshold above preindustrial would lead to the near-complete loss of the Greenland Ice Sheet over a millennium or more, causing a global mean sea level rise of up to 7 m. Current estimates indicate that the threshold is greater than 1°C but less than 4°C global mean warming with respect to preindustrial, but *confidence* is *low*. {5.8.1, 13.4.3, 13.4.4}

- Methods to counter climate change, termed geoengineering, have been proposed. Carbon dioxide removal (CDR) methods have biogeochemical and technological limitations to their potential on a global scale. There is insufficient knowledge to quantify how much CO_2 emissions could be reduced through negative emissions on a human timescale. Modelling shows that some solar radiation management (SRM) methods have the potential to substantially offset a global temperature rise, but they would also modify the global water cycle, and would not compensate for ocean acidification. If SRM were terminated for any reason, there is *high confidence* that global surface temperatures would rise very rapidly to values consistent with the greenhouse gas forcing. CDR and SRM methods carry unintended side effects and long-term consequences on a global scale. Limited evidence precludes a comprehensive quantitative assessment of both SRM and CDR and their impact on the climate system. {6.5, 7.7}

Box SPM.1: Representative Concentration Pathways (RCPs)

Climate change projections require information about future emissions or concentrations of greenhouse gases, aerosols and other anthropogenic drivers. This information is expressed as different scenarios of human activity, which are not assessed in this report. Climate change projections in this report are often reported conditional on a specific scenario, or a set of scenarios. The scenarios do not include trends in natural drivers such as solar or volcanic forcing.

For the Fifth Assessment Report of IPCC, the scientific community has defined a set of four new scenarios, referred to as the Representative Concentration Pathways (RCP). They are identified by their year 2100 total radiative forcing, ranging from approximately 2.6 W m^{-2} for RCP2.6 to 8.5 W m^{-2} for RCP8.5. The RCPs can contain 21st century climate policies and thus are framed differently compared to the no-climate policy scenarios used in previous assessment reports. For RCP6.0, and RCP8.5, radiative forcing does not peak by year 2100, whereas it does for RCP2.6 and RCP4.5, before declining (RCP2.6) or stabilizing (RCP4.5). While the RCPs span a wide range of total forcing values, they do not span the full range of plausible emissions in the literature, particularly for aerosols. Each RCP provides comprehensive high spatial resolution data sets of land use change, sector-based emissions of air pollutants, and both emissions and concentrations of greenhouse gases up to 2100, obtained from a combination of integrated assessment models, simple climate models, atmospheric chemistry and global carbon cycle models.

Most of the Coupled Model Intercomparison Project Phase 5 (CMIP5) simulations with comprehensive climate models and Earth System Models (ESMs) are performed with prescribed CO_2 concentrations reaching about 421 ppm (RCP2.6), 538 ppm (RCP4.5), 670 ppm (RCP6.0), and 936 ppm (RCP 8.5) by the year 2100. For RCP8.5, additional CMIP5 ESM simulations are performed with prescribed CO_2 emissions as provided by the integrated assessment models. These simulations enable investigation of uncertainties related to carbon cycle feedbacks.

The “label” associated with the 2100 forcing value of each RCP should be understood as indicative only, as the climate forcing resulting from all drivers varies between models due to specific model characteristics.

Tables

Table SPM.1: Extreme weather and climate events: Global-scale assessment of recent observed changes, human contribution to the changes, and projected further changes for the early (2016–2035) and late (2081–2100) 21st century. Bold indicates where the AR5 (black) provides a revised* global-scale assessment from the SREX (blue) or AR4 (red). Projections for early 21st century were not provided in previous assessment reports. Projections in the AR5 are relative to the reference period of 1986–2005, and use the new RCP scenarios.

Phenomenon and direction of trend	Assessment that changes occurred (typically since 1950 unless otherwise indicated)	Assessment of a human contribution to observed changes	Likelihood of further changes	
			Early 21st century	Late 21st century
Warmer and/or fewer cold days and nights over most land areas	*Very likely* [2.6.1] *Very likely* *Very likely*	***Very likely*** [10.6.1] *Likely* *Likely*	*Likely* [11.3.2] – –	*Virtually certain* [12.4.3] *Virtually certain* *Virtually certain*
Warmer and/or more frequent hot days and nights over most land areas	*Very likely* [2.6.1] *Very likely* *Very likely*	***Very likely*** [10.6.1] *Likely* *Likely* (nights only)	*Likely* [11.3.2] – –	*Virtually certain* [12.4.3] *Virtually certain* *Virtually certain*
Warm spells/heat waves. Frequency and/or duration increases over most land areas	***Medium confidence*** on a global scale *Likely* in some regions (a) [2.6.1] *Medium confidence in many (but not all) regions* *Likely*	***Likely*** (b) [10.6.2] *Not formally assessed* *More likely than not*	Not formally assessed (c) [11.3.2] – –	*Very likely* [12.4.3] *Very likely* *Very likely*
Heavy precipitation events. Increase in the frequency, intensity, and/or amount of heavy precipitation.	*Likely* more land areas with increases than decreases *Very likely* in central North America [2.6.2] *Likely* more land areas with increases than decreases *Likely over most land areas*	***Medium confidence*** [7.6.5, 10.6.1] *Medium confidence* *More likely than not*	*Likely* over many land areas [11.3.2] – –	***Very likely*** in some areas (d) [12.4.5] *Likely* over many areas *Very likely over most land areas*
Increases in intensity and/or duration of drought	***Low confidence*** on a global scale *Likely* changes in some regions (e) [2.6.2] *Medium confidence* in some regions *Likely* in many regions, since 1970 (f)	***Low confidence*** [10.6.1] *Medium confidence* *More likely than not*	*Low confidence* (g) [11.3.2] – –	***Likely*** *(medium confidence)* on a regional to global scale (h) [12.4.5] *Medium confidence* in some regions *Likely* (f)
Increases in intense tropical cyclone activity	***Low confidence*** in long term (centennial) changes *Virtually certain* in North Atlantic since 1970 [2.6.3] *Low confidence* *Likely* (in some regions, since 1970)	***Low confidence*** [10.6.1] *Low confidence* *More likely than not*	*Low confidence* [11.3.2] – –	***More likely than not*** in some basins [14.6] *More likely than not* in some basins *Likely*
Increased incidence and/or magnitude of extreme high sea level	*Likely* (since 1970) [3.7.5] *Likely* (late 20th century) *Likely*	Not assessed *Likely* (i) *More likely than not* (i)	Not assessed – –	***Very likely*** [13.7.2] *Very likely* (j) *Likely*

* The direct comparison of assessment findings between reports is difficult. For some climate variables, different aspects have been assessed, and the revised guidance note on uncertainties has been used for the SREX and AR5. The availability of new information, improved scientific understanding, continued analyses of data and models, and specific differences in methodologies applied in the assessed studies, all contribute to revised assessment findings.

Notes:
(a) *Likely* that heat wave frequency has increased in large parts of Europe, Asia and Australia.
(b) Attribution is based on available case studies. It is *likely* that human influence has substantially increased the probability of occurrence of some observed heat waves in some locations.
(c) Models project near-term increases in the duration, intensity and spatial extent of heat waves and warm spells.
(d) *Very likely* over most of the mid-latitude land-masses and over wet tropical regions.
(e) The frequency and intensity of drought has *likely* increased in the Mediterranean and West Africa and *likely* decreased in central North America and north-west Australia.
(f) AR4 assessed the area affected by drought.
(g) There is *low confidence* in projected changes in soil moisture.
(h) Regional to global-scale projected decreases in soil moisture and increased agricultural drought are *likely (medium confidence)* in presently dry regions by the end of this century under the RCP8.5 scenario. Soil moisture drying in the Mediterranean, Southwest US and southern African regions is consistent with projected changes in Hadley circulation and increased surface temperatures, so there is *high confidence* in *likely* surface drying in these regions by the end of this century under the RCP8.5 scenario.
(i) Attribution is based on the close relationship between observed changes in extreme and mean sea level.
(j) SREX assessed it to be *very likely* that mean sea level rise will contribute to future upward trends in extreme coastal high water levels.

Table SPM.2: Projected change in global mean surface air temperature and global mean sea level rise for the mid- and late 21st century. {12.4.1; Table 12.2, Table 13.5}

		2046–2065		2081–2100	
Variable	**Scenario**	mean	*likely* range [c]	mean	*likely* range [c]
Global Mean Surface Temperature Change (°C) [a]	RCP2.6	1.0	0.4 to 1.6	1.0	0.3 to 1.7
	RCP4.5	1.4	0.9 to 2.0	1.8	1.1 to 2.6
	RCP6.0	1.3	0.8 to 1.8	2.2	1.4 to 3.1
	RCP8.5	2.0	1.4 to 2.6	3.7	2.6 to 4.8
		mean	*likely* range [d]	mean	*likely* range [d]
Global Mean Sea Level Rise (m) [b]	RCP2.6	0.24	0.17 to 0.31	0.40	0.26 to 0.54
	RCP4.5	0.26	0.19 to 0.33	0.47	0.32 to 0.62
	RCP6.0	0.25	0.18 to 0.32	0.47	0.33 to 0.62
	RCP8.5	0.29	0.22 to 0.37	0.62	0.45 to 0.81

Notes:

(a) Based on the CMIP5 ensemble; anomalies calculated with respect to 1986–2005. Using HadCRUT4 and its uncertainty estimate (5−95% confidence interval), the observed warming to the reference period 1986−2005 used for projections is 0.61 [0.55 to 0.67] °C for 1850−1900, 0.30 [0.27 to 0.33] °C for 1961−1990, and 0.11 [0.09 to 0.13] °C for 1980−1999. {2.4.3; Tables 12.2 and 12.3}

(b) Based on 21 CMIP5 models; anomalies calculated with respect to 1986–2005. Where CMIP5 results were not available for a particular AOGCM and scenario, they were estimated as explained in Chapter 13, Table 13.5. The contributions from ice sheet rapid dynamical change and anthropogenic land water storage are treated as having uniform probability distributions, and as largely independent of scenario. This treatment does not imply that the contributions concerned will not depend on the scenario followed, only that the current state of knowledge does not permit a quantitative assessment of the dependence. Based on current understanding, only the collapse of marine-based sectors of the Antarctic Ice Sheet, if initiated, could cause global mean sea level to rise substantially above the *likely* range during the 21st century. There is *medium confidence* that this additional contribution would not exceed several tenths of a meter of sea level rise during the 21st century.

(c) Calculated from projections as 5−95% model ranges. These ranges are then assessed to be *likely* ranges after accounting for additional uncertainties or different levels of confidence in models. For projections of global mean surface temperature change in 2046−2065 *confidence* is *medium*, because contributions of radiative forcing and initial conditions to the temperature response uncertainty are larger than for 2081−2100. The likely ranges for 2046−2065 do not take into account the possible influence of factors that lead to near-term (2016−2035) projections of global mean surface temperature that are lower than the 5−95% model ranges, because the influence of these factors on longer term projections has not been quantified because of insufficient scientific understanding. {11.3.6}

(d) Calculated from projections as 5−95% model ranges. These ranges are then assessed to be *likely* ranges after accounting for additional uncertainties or different levels of confidence in models. For projections of global mean sea level rise *confidence* is *medium* for both time horizons.

Figures

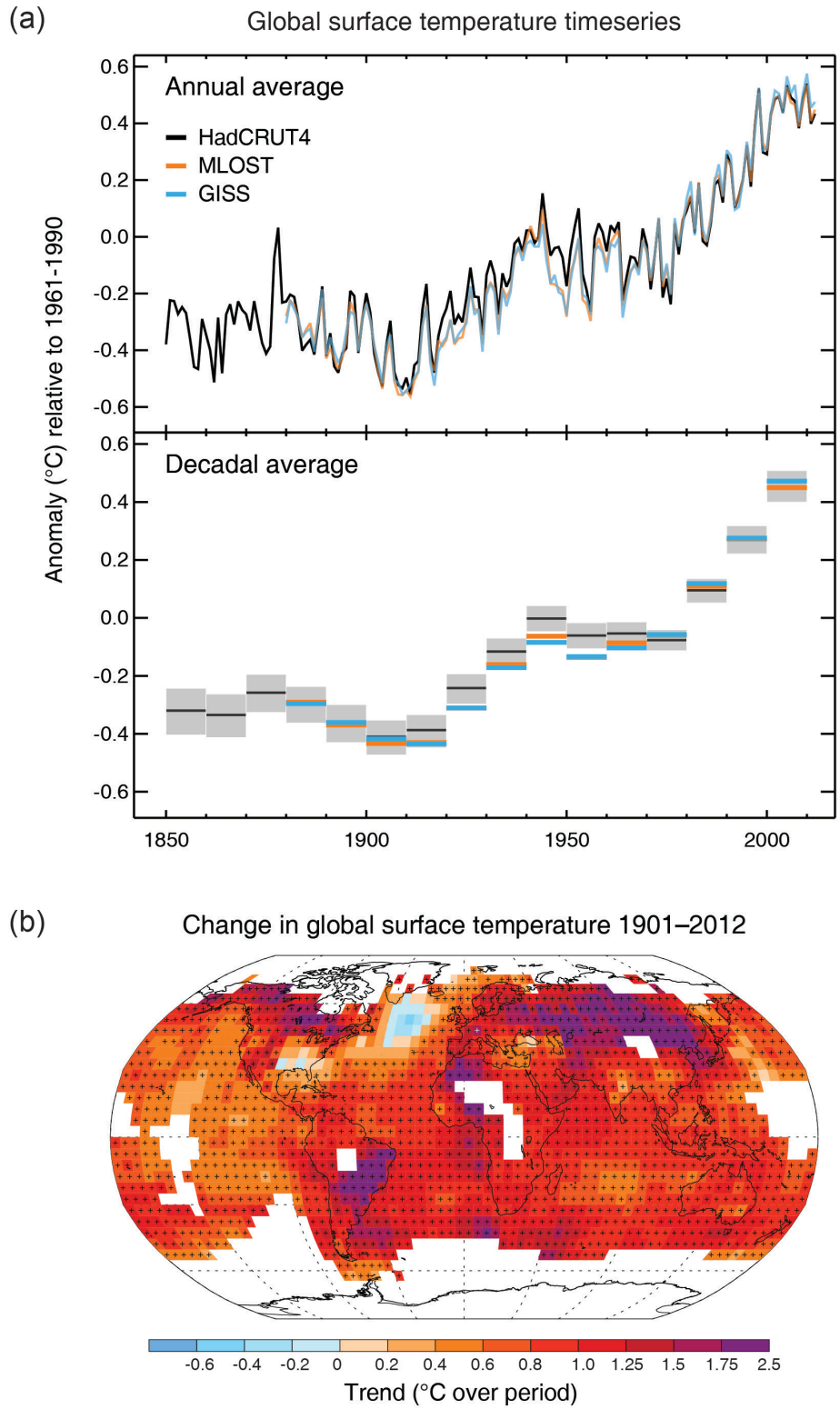

Figure SPM.1: (a) Observed global mean combined land and ocean temperature anomalies from three surface temperature data sets (black – HadCRUT4, yellow – MLOST, blue – GISS). Top panel: annual mean values, bottom panel: decadal mean values including the estimate of uncertainty for HadCRUT4. Anomalies are relative to the mean of 1961−1990. (b) Map of the observed temperature change from 1901−2012derived from temperature trends determined by linear regression of the MLOST time series. Trends have been calculated only for grid boxes with greater than 70% complete records and more than 20% data availability in the first and last 10% of the time period. Grid boxes where the trend is significant at the 10% level are indicated by a + sign. {Figures 2.19–2.21; Figure TS.2}

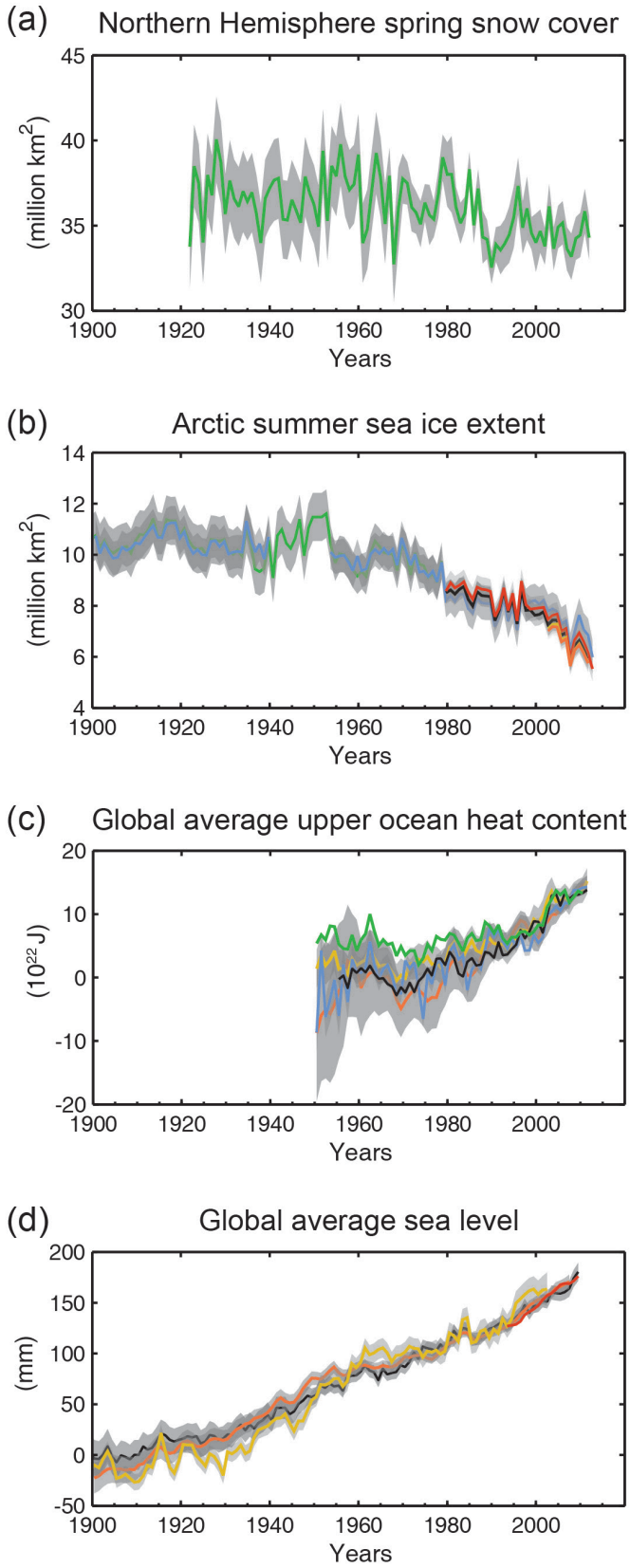

Figure SPM.2: Multiple observed indicators of a changing global climate: (a) Northern Hemisphere March-April average snow cover extent, (b) Arctic July-August-September average sea ice extent, (c) change in global mean upper ocean heat content normalized to 2006−2010, and relative to the mean of all datasets for 1971, (d) global mean sea level relative to the 1900–1905 mean of the longest running dataset, and with all datasets aligned to have the same value in 1993, the first year of altimetry data. All time-series (coloured lines) show annual values, and where assessed, uncertainties are indicated by different shades of grey. See Chapter 2, Supplementary Material 2.SM.5 for a listing of the datasets. {Figures 3.2, 3.13, 4.19, and 4.3; FAQ 2.1, Figure 2; Figure TS.1}

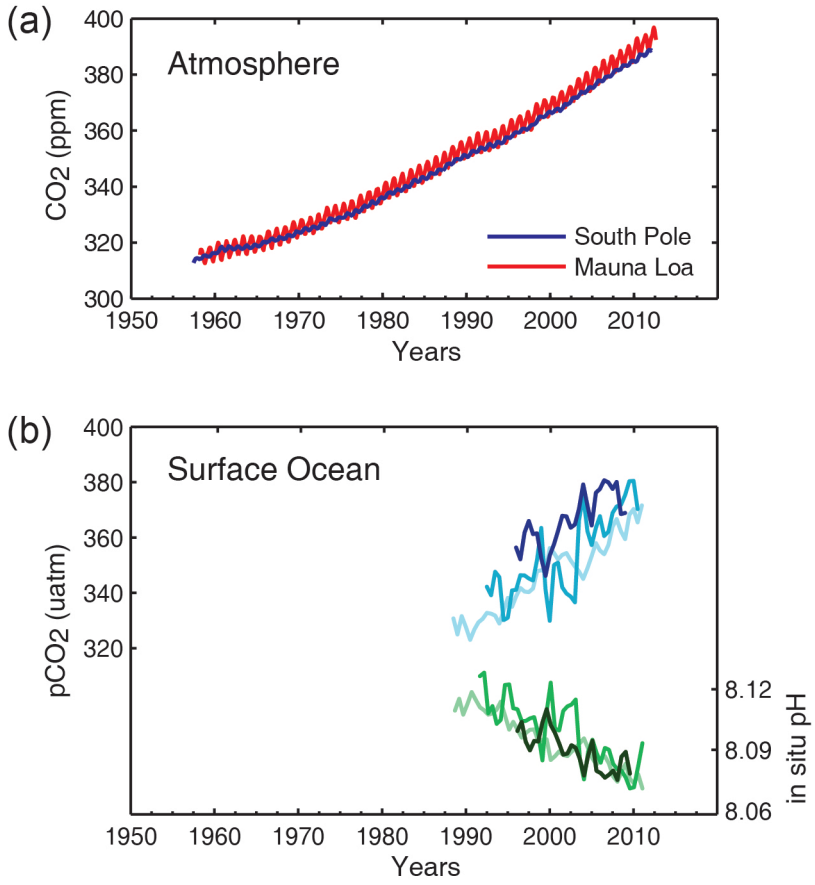

Figure SPM.3: Multiple observed indicators of a changing global carbon cycle. Measurements of atmospheric concentrations of carbon dioxide (CO_2) are from Mauna Loa and South Pole since 1958. Measurements of partial pressure of CO_2 at the ocean surface are shown from three stations from the Atlantic (29°10′N, 15°30′W – dark blue/dark green; 31°40′N, 64°10′W – blue/green) and the Pacific Oceans (22°45′N, 158°00′W − light blue/light green), along with the measurement of in situ pH, a measure of the acidity of ocean water (smaller pH means greater acidity). Full details of the datasets shown here are provided in the underlying report. {Figures 2.1 and 3.17; Figure TS.5}

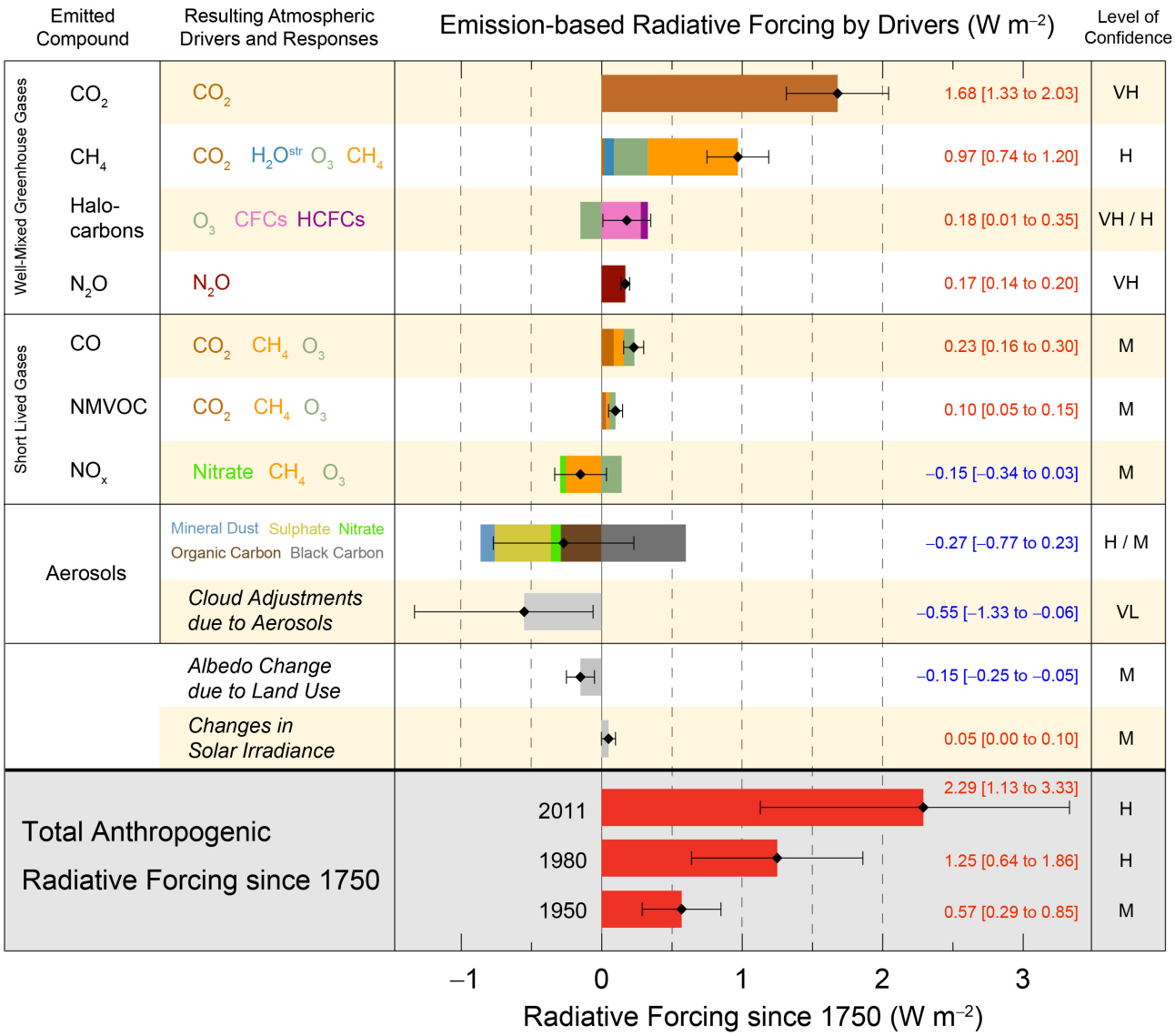

Figure SPM.4: Radiative forcing estimates with respect to 1750 and uncertainties for the main drivers of climate change. Values are global average radiative forcing (RF, see [8]) partitioned according to the emitted compounds or processes that result in a combination of drivers. The best estimates of the net radiative forcing is shown as a black diamond with corresponding uncertainty intervals; the numerical values are provided on the right of the figure, together with the confidence level (VH – *very high*, H – *high*, M – *medium*, L – *low*, VL – *very low*). For halocarbons, confidence is H for ozone, and VH for CFCs and HCFCs. For aerosols, confidence is H for total aerosols, and M for individual aerosol components. Aerosol forcing other than cloud adjustments is the −0.27 W m^{-2} shown in the bar above and the −0.04 W m^{-2} from the nitrate response to NO_x emissions (which is equal to the −0.35 W m^{-2} due to aerosol-radiation interactions plus +0.04 W m^{-2} due to black carbon on snow), while the cloud adjustment term includes a response of −0.1 W m^{-2} due to aerosol-radiation interactions which is attributable to black carbon and −0.45 W m^{-2} that has not been attributed to individual components. Small forcings due to contrails, volcanoes, HFCs, PFCs and SF_6 are not shown. Total anthropogenic radiative forcing is provided for three different years with respect to 1750. {Figures 8.16 and 8.18; Figures TS.6 and TS.7}

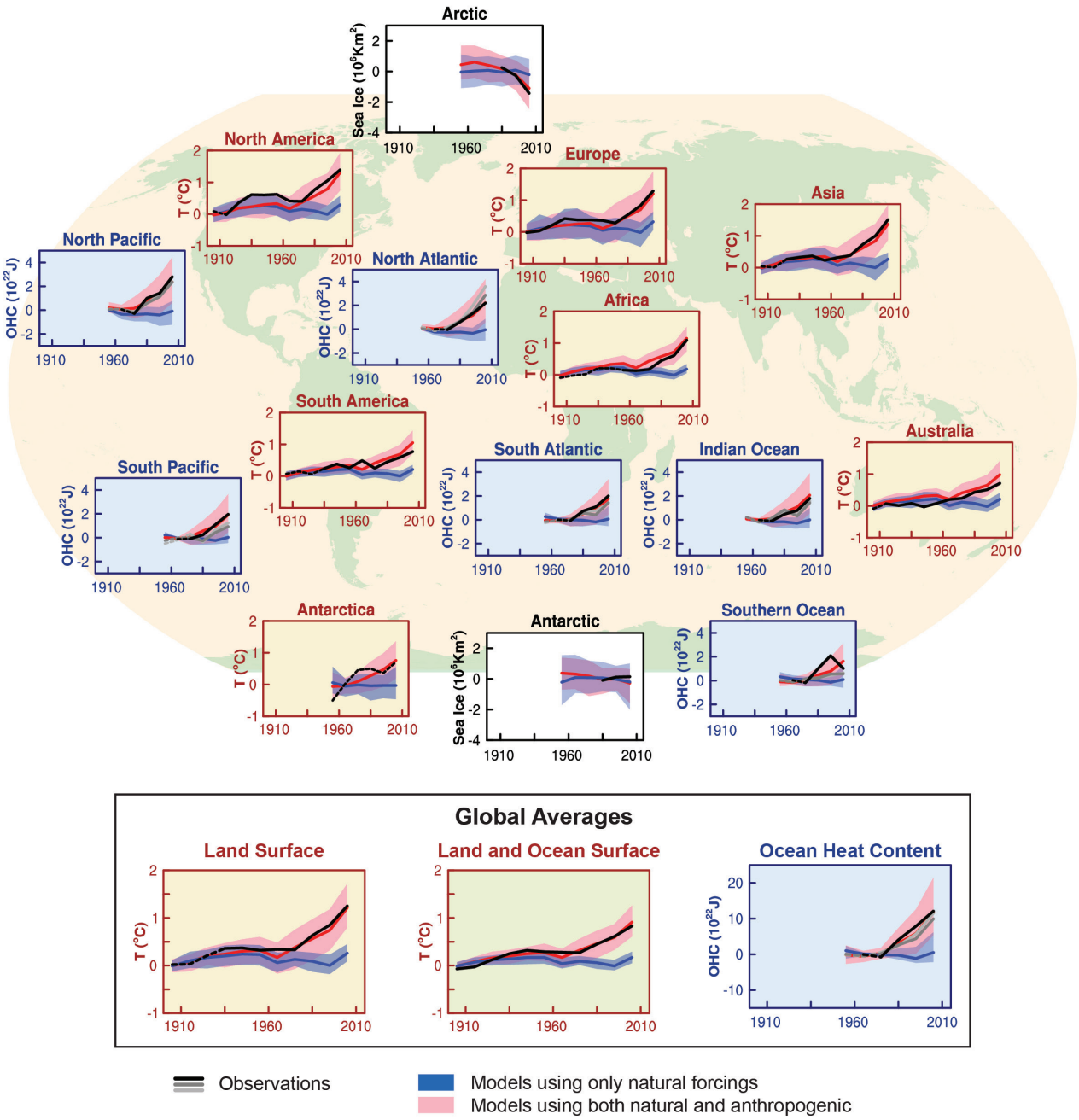

Figure SPM.5: Comparison of observed and simulated climate change based on time-series of three large-scale indicators in the atmosphere, the cryosphere and the ocean: continental land surface air temperatures (yellow panels), Arctic and Antarctic sea ice (white panels), ocean heat uptake in the major ocean basins (blue panels). Global average changes are also given. All time-series are decadal averages, plotted at the centre of the decade. For temperature panels, observations are dashed lines if the spatial coverage of areas being examined is below 50%. For ocean heat content and sea ice panels the solid line is where the coverage of data is good and higher in quality, and the dashed line is where the data coverage is only adequate, and thus, uncertainty is larger. Model results shown are CMIP5 multi-model means and ensemble ranges, with shaded bands indicating the 5 to 95% confidence intervals[13]. See Chapter 10, Supplementary Material 10.SM.1 for datasets and methods used. {Figure 10.21; Figure TS.12}

[13] For surface temperature, the blue shaded band is based on 52 simulations from 17 climate models using only natural forcings, while the red shaded band is based on 147 simulations from 44 climate models using natural and anthropogenic forcings. For ocean heat content, 10 simulations from 10 models, and 13 simulations from 13 models were used respectively. For sea ice extent, a subset of models are considered that simulated the mean and seasonal cycle of the sea ice extent within 20% of the observed sea-ice climatology for the period 1981–2005 (Arctic: 24 simulations from 11 models for both red and blue shaded bands, Antarctic: 21 simulations from 6 models for both red and blue shaded bands).

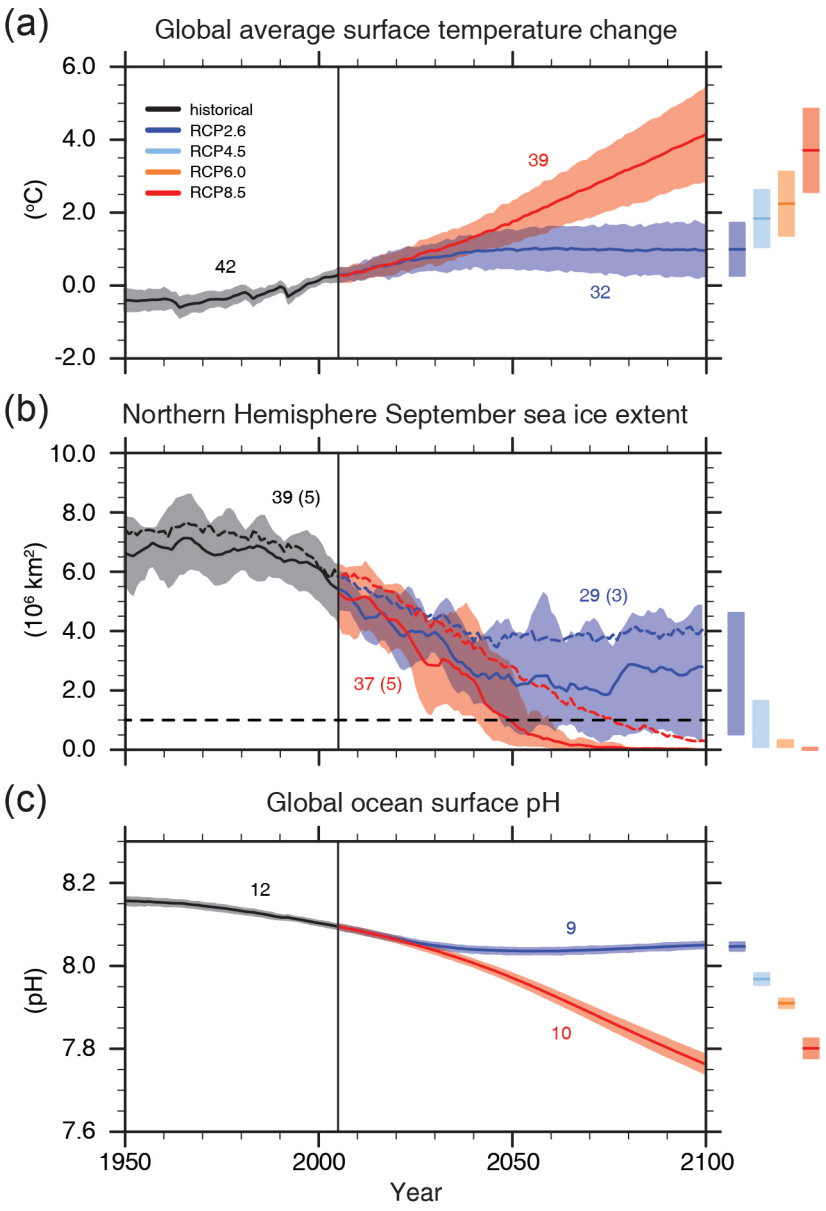

Figure SPM.6: CMIP5 multi-model simulated time series from 1950 to 2100 for (a), change in global annual mean surface temperature relative to 1986–2005, see Table SPM.2 and footnote 9 for other reference periods. (b), Northern Hemisphere sea ice extent in September (5 year running mean), and (c), global mean ocean surface pH. Time series of projections and a measure of uncertainty (shading, minimum-maximum range) are shown for scenarios RCP2.6 (blue) and RCP8.5 (red). Black (grey shading) is the modelled historical evolution using historical reconstructed forcings. The mean and associated uncertainties averaged over 2081−2100 are given for all RCP scenarios as colored vertical bars. The numbers of CMIP5 models used to calculate the multi-model mean is indicated. For sea ice extent (b), the projected mean and uncertainty (minimum-maximum range) of the subset of models that most closely reproduce the climatological mean state and 1979–2012 trend of the Arctic sea ice is given. For completeness, the CMIP5 multi-model mean is indicated with dashed lines. {Figures 6.28, 12.5, and 12.28–12.31; Figures TS.15, TS.17, and TS.20}

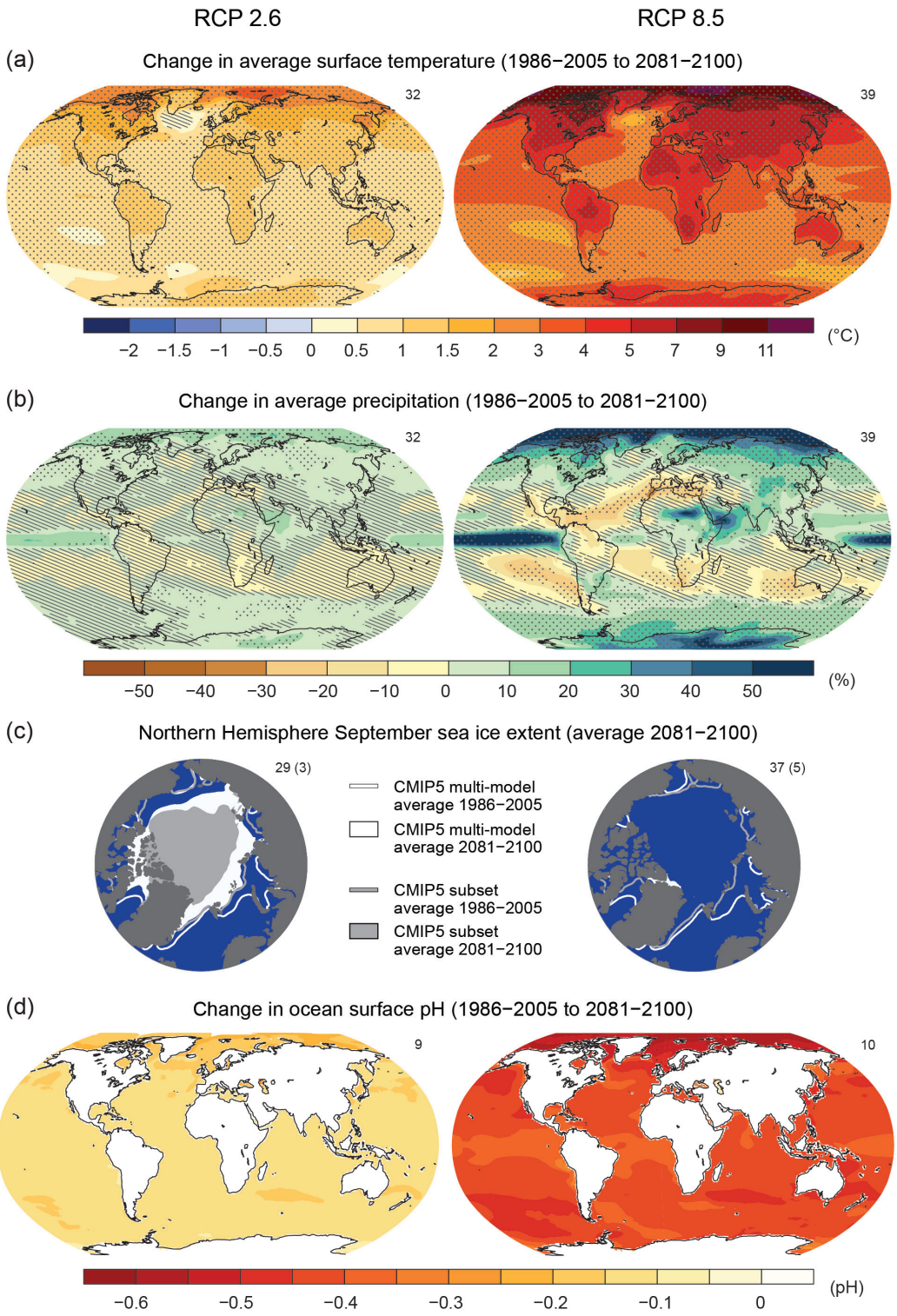

Figure SPM.7: Maps of CMIP5 multi-model mean results for the scenarios RCP2.6 and RCP8.5 in 2081–2100 of (a), surface temperature change, (b), average percent change in mean precipitation, (c), Northern Hemisphere September sea ice extent, and (d) change in ocean surface pH. Changes in panels (a), (b) and (d) are shown relative to 1986–2005. The number of CMIP5 models to calculate the multi-model mean is indicated in the upper right corner of each panel. For panels (a) and (b), hatching indicates regions where the multi model mean is less than one standard deviation of internal variability. Stippling indicates regions where the multi model mean is greater than two standard deviations of internal variability and where 90% of models agree on the sign of change (see Box 12.1). In panel (c), the lines are the modeled means for 1986−2005; the filled areas are for the end of the century. The CMIP5 multi-model mean is given in white color, the projected mean sea ice extent of a subset of models that most closely reproduce the climatological mean state and 1979–2012 trend of the Arctic sea ice cover is given in grey color. {Figures 6.28, 12.11, 12.22, and 12.29;Figures TS.15, TS.16, TS.17, and TS.20}

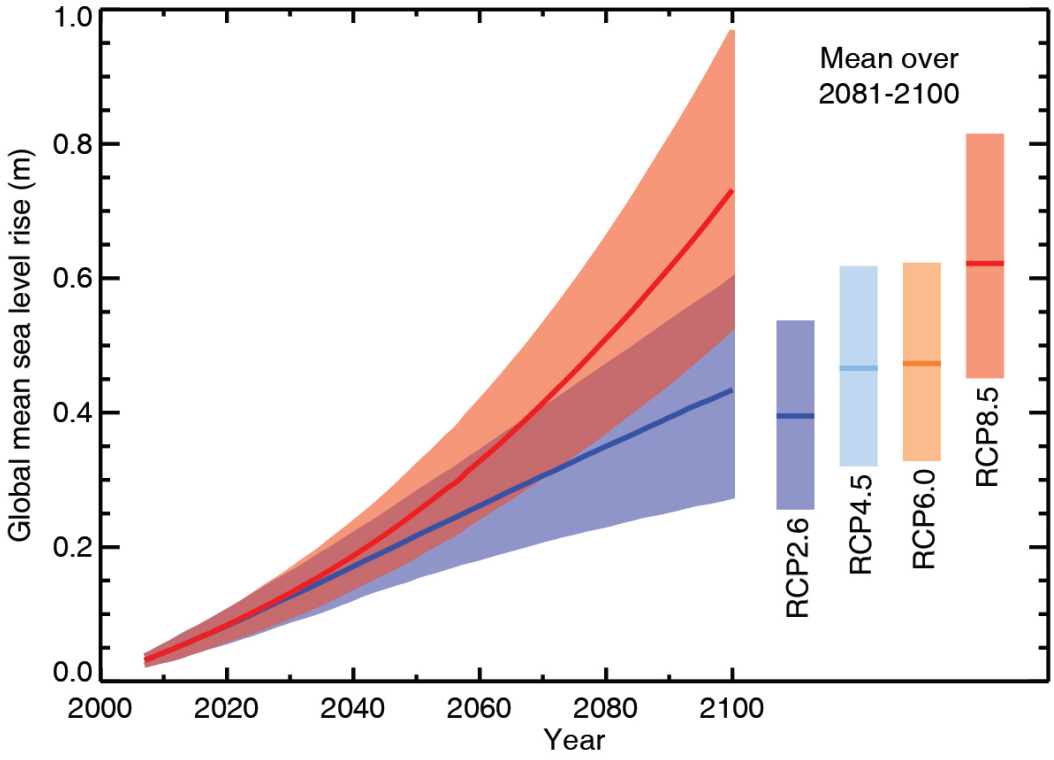

Figure SPM.8: Projections of global mean sea level change over the 21st century relative to 1986−2005 from the combination of CMIP5 and process-based models, for the two emissions scenarios RCP2.6, and RCP8.5. The assessed *likely* range is shown as a shaded band. The assessed *likely* ranges for the mean over the period 2081−2100 for all RCP scenarios are given as coloured vertical bars, with the corresponding median value given as a horizontal line. Based on current understanding, only the collapse of marine-based sectors of the Antarctic ice sheet, if initiated, could cause global mean sea level to rise substantially above the *likely* range during the 21st century. However, there is *medium confidence* that this additional contribution would not exceed several tenths of a meter of sea level rise during the 21st century. {Table 13.5, Figures13.10 and 13.11; Figures TS.21 and TS.22}

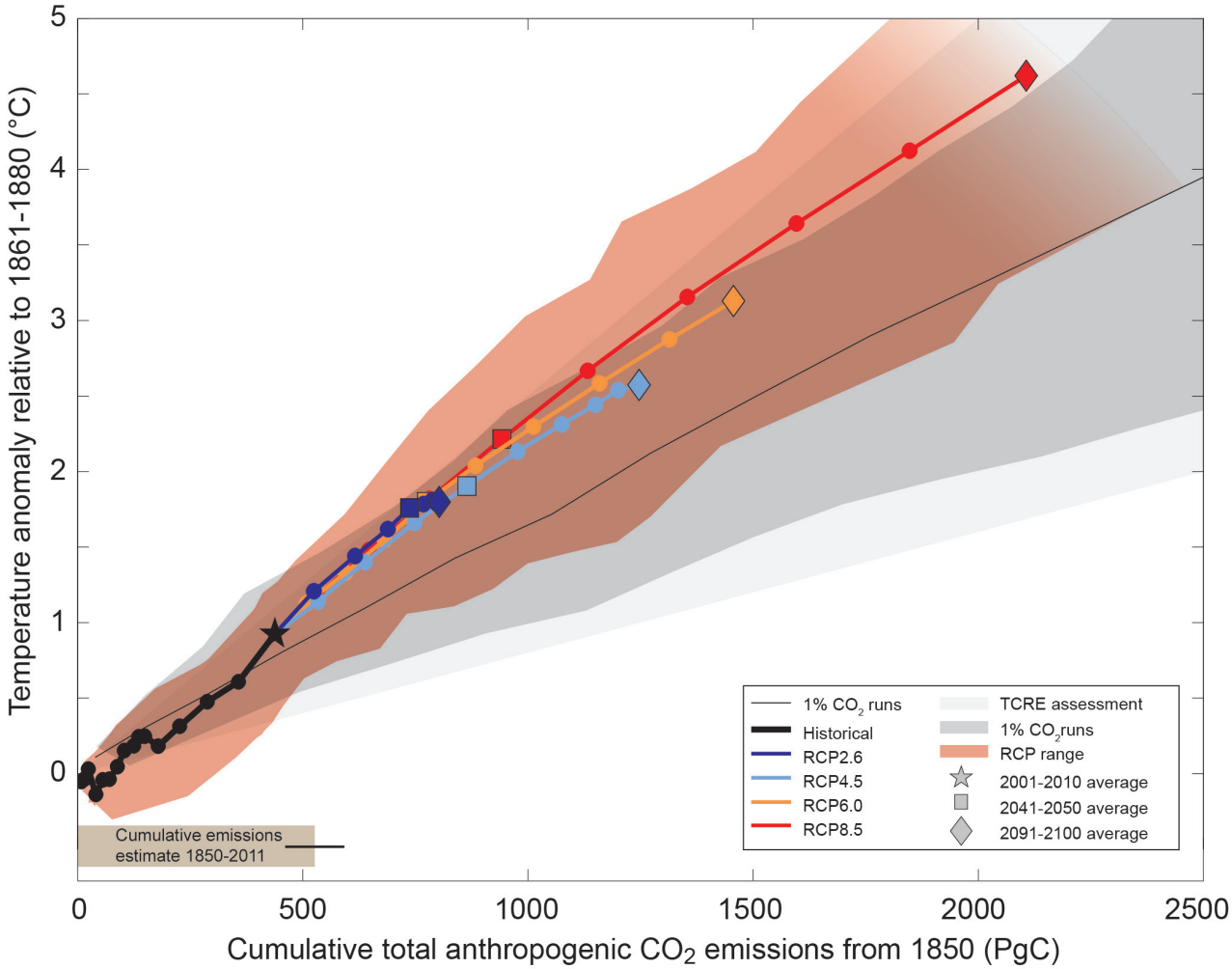

Figure SPM.9: Global mean temperature increase as a function of cumulative total global CO_2 emissions from various lines of evidence. Multi-model results from a hierarchy of climate-carbon cycle models for each RCP until 2100 shown with coloured lines and decadal means (dots). The decadal means for 2001−2010 (star), 2041−2050 (square) and 2091−2100, (diamond) are highlighted. Model results over the historical period (1860–2010) are indicated in black. The coloured plume illustrates the multi-model spread over the four RCP scenarios and fades with the decreasing number of available models. The multi-model mean and range simulated by CMIP5 models, forced by a CO_2 increase of 1% per year, is given by the thin black line and dark grey area. The light grey wedge represents this report's assessment of the transient climate response to emissions (TCRE) from CO_2 only. All values are given relative to the 1861−1880 base period. The horizontal brown bar and solid black line at the bottom-left illustrate the assessment of total cumulative carbon emissions until 2011 with associated uncertainties. All time-series are represented by connecting decadal averages to illustrate the long-term trends. {Figure 12.45; TFE.8, Figure 1}